DOKUZ EYLÜL UNIVERSITY

GRADUATE SCHOOL OF NATURAL AND APPLIED SCIENCES

REGRESSION CONTROL CHART FOR AUTOCORRELATED DATA

by

Aslan Deniz KARAOĞLAN

May, 2010

İZMİR

REGRESSION CONTROL CHART FOR AUTOCORRELATED DATA

A Thesis Submitted to the
Graduate School of Natural and Applied Sciences of Dokuz Eylül University
In Partial Fulfillment of the Requirements for the Degree of Doctor of Philosophy in Industrial Engineering, Industrial Engineering Program

by

Aslan Deniz KARAOĞLAN

May, 2010
İZMİR

Ph.D. THESIS EXAMINATION RESULT FORM

We have read the thesis entitled **"REGRESSION CONTROL CHART FOR AUTOCORRELATED DATA"** completed by **ASLAN DENİZ KARAOĞLAN** under supervision of **PROF. DR. GÜNHAN MİRAÇ BAYHAN** and we certify that in our opinion it is fully adequate, in scope and in quality, as a thesis for the degree of Doctor of Philosophy.

Prof. Dr. G. Miraç BAYHAN

Supervisor

Prof. Dr. Nihat BADEM	Prof. Dr. Mine DEMİRSOY
Thesis Committee Member	Thesis Committee Member
Assoc. Prof. Dr. Aşkıner GÜNGÖR	Assist. Prof. Dr. Mehmet ÇAKMAKÇI
Examining Committee Member	Examining Committee Member

Prof. Dr. Mustafa SABUNCU
Director
Graduate School of Natural and Applied Sciences

ACKNOWLEDGMENTS

First and foremost I would like to express my deep gratitude and thanks to my advisor Prof. Dr. G. Miraç BAYHAN for her continuous support, guidance, and valuable advice throughout the progress of this dissertation.

I sincerely acknowledge and thank the members of my thesis committee, Prof. Dr. Nihat BADEM and Prof. Dr. Mine DEMİRSOY, for their helpful comments, encouragement, and suggestions.

I would also like to thank my friends Sabri BİCAKCI, Barış ÖZKUL and all my friends for their support, encouragement, and friendship.

I would like to express my thanks to all the professors and colleagues in the Department of Industrial Engineering for their support and encouragement.

Finally, I would like to express my indebtedness and many thanks to my wife Arzu KARAOĞLAN and my parents, Hamit and Gülten KARAOĞLAN, and my sister Derya for their love, confidence, encouragement and endless support in my whole life.

Aslan Deniz KARAOĞLAN

REGRESSION CONTROL CHART FOR AUTOCORRELATED DATA

ABSTRACT

With the growing of automation in manufacturing, process quality characteristics are being measured at higher rates and data are more likely to be autocorrelated. The residual charts or control charts with modified control limits for autocorrelated data are widely used approaches for statistical process monitoring in the case of autocorrelated process data. Data sets collected from industrial processes may have both a particular type of trend and autocorrelation among adjacent observation. To the best of our knowledge there are not any schemes that monitor autocorrelated and trending process observations directly to detect the mean shift in the process observations. In this thesis, a new regression control chart which is able to detect the mean shift in a production process is presented. This chart is designed for autocorrelated process observations having a linearly increasing trend. Existing approaches may individually cope with autocorrelated or trending data. The proposed chart requires the identification of trend stationary first order autoregressive (trend AR(1) for short) model as a suitable time series model for process observations. In this thesis an integrated neural network structure, which is composed of appropriate number of linear vector quantization networks, multi layer perceptron networks, and Elman networks, is proposed to recognize the autocorrelated and trending patterns. The neural based system performance is evaluated in terms of the classification rate. After recognizing the trending and autocorrelated data by means of neural networks, proposed modified regression control chart for autocorrelated data is used for different magnitudes of the process mean shift, under the presence of various levels of autocorrelation, to determine whether the trending and autocorrelated process is in-control or not. The performance of proposed chart is evaluated in terms of the accurate signal rate and the average run length.

Keywords: Statistical process control, Regression control chart, Artificial neural network (ANN), Autocorrelated processes, Pattern recognition, Trend AR(1) model.

OTOKORELASYONLU GÖZLEMLER İÇİN REGRESYON KONTROL KARTI

ÖZ

Üretimde otomasyonun gelişmesiyle birlikte, süreç kalite karakteristikleri daha yüksek oranlarda ölçülmekte ve veriler çoğunlukla otokorelasyonlu olmaktadır. Residual kartları veya otokorelasyonlu veriler için modifiye edilmiş limitli kontrol kartları otokorelasyonlu süreç verilerinin istatistiksel süreç kontrolünde yaygın olarak kullanılan yaklaşımlardır. Endüstriyel süreçlerden toplanan veriler hem belirli bir trende hem de ardışık gözlemler arası otokorelasyona sahip olabilir. Otokorelasyonlu ve trend gösteren süreç gözlemlerinin ortalamadan sapmalarını tespit etmek için gözlemleri direkt olarak görüntüleyen bir kartın mevcut olduğuna ilişkin bir bilgiye sahip değiliz. Bu tezde üretim sürecinde meydana gelen ortalamadan sapmaları teşhiş edebilen yeni bir regresyon kontrol kartı sunulmaktadır. Bu kart doğrusal artan trend gösteren otokorelasyonlu gözlemler için tasarlanmıştır. Eski yöntemler otokorelasyonlu ve trend gösteren verilerle ayrı ayrı uğraşmaktadır. Önerilen kart süreç gözlemleri için uygun zaman serisi modeli olarak trend durağan birinci dereceden otoregresif (kısaca Trend AR(1)) modelin tanınmasını gerektirir. Bu tezde ayrıca trend gösteren otokorelasyonlu örüntülerin tanınmasında kullanılmak üzere uygun sayıda doğrusal vektör parçalama ağları, çok katmanlı algılayıcı ağları ve Elman ağlarından oluşan bütünleşik ağ yapısı önerilmektedir. Önerilen yapay sinir ağı tabanlı sistemin performansı doğru sınıflandırma yüzdesine göre değerlendirilmektedir. Trend gösteren otokorelasyonlu verilerin yapay sinir ağları yardımıyla teşhisinden sonra, otokorelasyonlu veriler için önerilen regresyon kontrol kartı, farklı seviyelerdeki otokorelasyonun varlığı altında farklı büyüklüklerdeki ortalamadan sapmalar için, trend gösteren otokorelasyonlu sürecin kontrol altında olup olmadığını belirlemek amacıyla kullanılmaktadır. Önerilen kartın performansı, doğru sinyal oranı ve ortalama koşum uzunluğu dikkate alınarak hesaplanmaktadır.

Anahtar sözcükler: İstatistiksel süreç kontrol, Regresyon kontrol kartı, Yapay sinir ağı (YSA), Otokorelasyonlu süreçler, Örüntü tanıma, Trend AR(1) model.

CONTENTS

Page

CHAPTER ONE

INTRODUCTION

In this chapter, the background, motivation and objectives of this work are stated, and the organization of this dissertation is outlined.

1.1 Background and Motivation

If a product is to meet customer requirements, generally it should be produced by a process that is stable or repeatable where the undesirable variability does not exists. More precisely, the process must be capable of operating with little variability around the target or nominal dimensions of the product's quality characteristics. Statistical process control (SPC) is a powerful collection of problem-solving tools useful in achieving process stability and improving capability through the reduction of variability. Control charts are statistical process control tools used to determine whether a process is in-control. Since the first control chart has been proposed by Shewhart in 1931, lots of charts have been developed and then improved to be used for different process data. In its basic form, a control chart compares process observations with a pair of control limits. The standard assumptions that are usually cited in justifying the use of control charts are that the data generated by the in-control process are normally and independently distributed. However the independency assumption is not realistic in practice. The most frequently reported effect on control charts of violating such assumptions is the erroneous assignment of the control limits. Most of the control chart applications displayed incorrect control limits and more than half of these displacements were due to violation of the independence assumption. Misplacement of control limits was due to serial correlation (i.e., autocorrelation) in the data. However, many processes such as those found in refinery operations, smelting operations, wood product manufacturing, waste-water processing and the operation of nuclear reactors have been shown to have autocorrelated observations.

When there is significant autocorrelation in a process, traditional control charts with iid (independent and identically distributed) assumption can still be used, but they will be ineffective. These charts will result with poor performance like high false alarm rates and slow detection of process shifts. Because of this reason some modifications for traditional control charts are necessary if autocorrelation cannot be ignored. Therefore, various control charts have been developed for monitoring autocorrelated processes. In the literature three general approaches are recommended for autocorrelated data: (i) fit ARIMA model to data and then apply traditional control charts such as Shewhart, cumulative sum (CUSUM), exponentially-weighted moving average (EWMA) to process residuals, (ii) monitor the autocorrelated process observations by modifying the standard control limits to account for the autocorrelation (iii) eliminate the autocorrelation by using an engineering controller (Montgomery, 1997).

A common approach to detect a possible process mean shift in the autocorrelated data is to use residual control charts, also known as the special cause chart (SCC), which are constructed by applying traditional SPC charts (Shewhart, CUSUM, EWMA, and etc.) to the residuals from a time series model of the process data (Zhang, 2000). In these charts, forecast errors, namely residuals, are assumed to be statistically uncorrelated. An appropriate time series model is fitted to the autocorrelated data and the residuals are plotted in a control chart. For this reason all of the well-known control schemes can be transformed to the residual control scheme. The main advantage of a residual chart is that it can be applied to any autocorrelated data whether the process is stationary or not. However, there are also some disadvantages such as time series modeling knowledge is needed for constructing the ARIMA model, and in addition, the detecting capability of the residual chart is not always great. In the relevant literature, to overcome the disadvantages of the residual control charts, modified control chart that is based on applying the original control chart methodology with a little modification is proposed. In this method, autocorrelated data is used in original control chart by adjusting its control limits. Modified control charts such as moving centerline exponentially-weighted moving average (MCEWMA), EWMA for stationary

process (EWMAST), autoregressive moving average (ARMA) and other control charts that were firstly proposed for autocorrelated process observations are widely employed to deal with the disadvantages of the residual charts for stationary autocorrelated process data (Montgomery, 1997). However, since rearrangement of the control limits for autocorrelated data is not so easy and application of modified charts is more complicated then the residual control charts.

On the other hand, if independent process data exhibit an underlying trend due to systemic causes, usually control charts based on ordinary least squares (OLS) regression are used for monitoring and control. Trends are usually due to gradual wearing out or deterioration of a tool or some other critical process components. In chemical processes linear trend often occurs because of settling or separation of the components of a mixture. They can also result from human causes, such as operator fatigue or the presence of supervision. Finally, trends can result from seasonal influences, such as temperature. The traditional control charts with horizontal control limits and a center line with a slope of zero have proven unreliable when systemic trend exists in process data. A device useful for monitoring and analyzing processes with trend is the regression control chart (see Mandel (1969)). A regression based control chart which is the combination of the conventional control chart and regression analysis is designed to control a varying (rather than a constant) average of trending process, and assumes that the values of the dependent variable are linearly (causally) related with the values of the independent variable. Rather than using standard control charts, practitioners typically implement regression based control charts to monitor a process with systemic trend (Utley & May, 2008). Quesenberry (1988) points out that these approaches essentially assume that resetting the process is expensive and that they attempt to minimize the number of adjustments made to keep the parts within specifications rather than reducing overall variability. However, since the Mandel's regression control chart was developed for independent data, it is not an effective tool for monitoring process shift in autocorrelated process observations.

In addition to autocorrelated or trended observations, many industrial processes give such data that exhibit both trend and autocorrelation among adjacent

observations. In other words the types of industrial series (especially chemical processes) frequently exhibit a particular kind of trend behavior, that can be represented by a trend stationary first order autoregressive (trend AR(1)) model. Much recent research has considered performance comparison of control charts for residuals of autocorrelated processes in terms of average run length (ARL) criterion, which is defined as the number of observations that must be plotted before a point indicates an out-of-control condition. Although we made a comprehensive review, there appears to be no chart that directly monitors the original data which exhibit both increasing linear trend and serial correlation. This observation has been the motivation for the present work on developing a new regression control chart that cope with autocorrelated observations (RCCA for short) in which observation values increase with respect to time. The RCCA requires the identification of trend AR(1) model as a suitable time series model for observations. In this thesis, for a wide range of possible shifts and autocorrelation coefficients, performance of the proposed chart is evaluated by simulation experiments. Average run length (ARL) and average correct signal rate are used as performance criteria.

1.2 Research Objective

In this thesis, it is aimed to develop a new regression control chart that can be used to detect the different magnitudes of the process mean shift, under the presence of various levels of autocorrelation in a process having both autocorrelated and trending data. By this way it is aimed to determine whether the given process is in-control or not. The specific approaches are as follows:

- To develop a new regression control chart that directly monitors the original data which exhibit both increasing linear trend and autocorrelation.

- To give a comprehensive literature review on the control charts for autocorrelated data.

- To propose an efficient neural network structure to recognize the autocorrelated and trending input patterns of proposed chart.

1.3 Organization of the Thesis

This dissertation is organized as follows. In chapter two, the basic concepts of statistical process control charts, autocorrelation and time series models are described. Then conventional regression control chart that is designed to control a varying (rather than a constant) average is discussed. Also, a review of the recent works on regression control charts and control chart applications in autocorrelated processes are given. Construction steps of the proposed regression control chart with an illustrative example are given in chapter three. Proposed neural network structure that is used for recognizing trending and autocorrelated patterns are presented in the same chapter. Performance evaluation of the proposed chart is given in chapter four. Finally, the conclusions are pointed out in chapter five.

CHAPTER TWO

STATISTICAL PROCESS CONTROL CHARTS

In this chapter, the basic concepts of statistical process control charts and definition of autocorrelation and time series models are given before examining control charts for autocorrelated data. Then conventional regression control chart is discussed. A review of the recent works on control chart applications in autocorrelated processes and regression control chart applications are also given in chronological order.

2.1 The Basic Concepts

If a product is to meet customer requirements, generally it should be produced by a process that is stable or repeatable where the undesirable variability does not exists. More precisely, the process must be capable of operating with little variability around the target or nominal dimensions of the product's quality characteristics. In any production process, regardless of how well designed or carefully maintained it is; a certain amount of inherent or natural variability will always exist. The sources of variability can be broken down into two main categories. Shewhart calls these categories *change* and *assignable causes*. Deming calls *common* and *special causes* of variability (Levine, Ramsey, & Berenson, 1995). If only common causes are operating on the system, the process is said to be in a state of statistical control. A process that is in a state of statistical control is considered to be stable. In another words, a stable process is in a state of statistical control and has only common causes of variability operating on it. Any attempt to make adjustment to a stable process and threat common causes as special causes constitutes tampering and will only result in increased variability. If special causes are operating, the system is considered to be out of statistical control and invertation or change permits reduction of process variability. In other words, a process is said to be out of statistical control if one or more special causes are operating on it (Levine, Ramsey, & Berenson, 1995).

A major objective of statistical process control is to quickly detect the occurrence of assignable causes of process shifts so that investigation of the process and corrective action may be undertaken before many nonconforming units are manufactured. The control chart is an on-line process control technique widely used for this purpose. Control charts may also be used to estimate the parameters of a production process, and through this information to determine process capability. The control chart may also provide information useful in improving the process. The eventual goal of statistical process control is the elimination of variability in the process. It may not be possible to completely eliminate variability, but the control chart is an effective tool in reducing variability as much as possible (Montgomery, 1997).

Run chart is basic form for control chart. A run chart, which is shown in Figure 2.1, is a very simple technique for analyzing the process in the development stage or, for that matter, when other charting techniques are not applicable. One danger of using a run chart is its tendency to show every variation in data as being important.

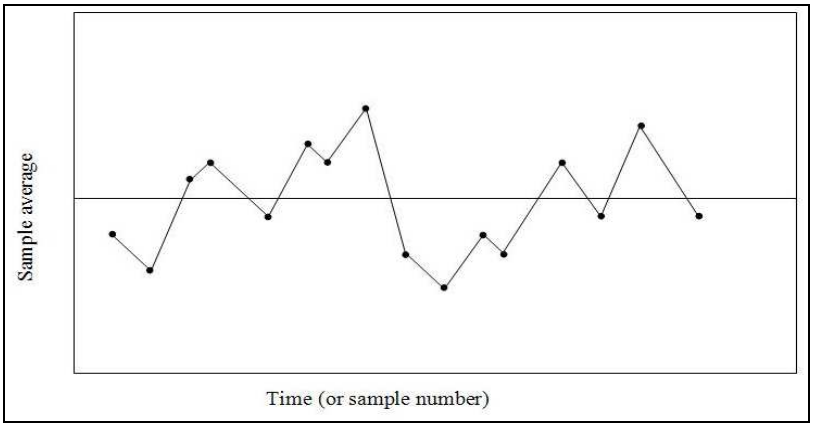

Figure 2.1 A typical run chart (Besterfield, Besterfield-Michna, Besterfield, & Besterfield-Sacre, 2003).

A control chart is a special type of run chart with limits. It shows the amount and nature of variations in the process over time. It also enables pattern interpretation and detection of changes in the process (Ross, 1999). In order to indicate when observed variations in quality are greater than could be left to change, the control chart method of analysis and representation of data is used. The control chart method for variables

is a means of visualizing the variations that occur in the central tendency and dispersion of a set of observations. It is a graphical record of the quality of a particular characteristic (Besterfield et al., 2003). A typical control chart is shown in Figure 2.2. This chart plots the averages of measurements of a quality characteristic in samples taken from the process versus time (or the sample number). The chart has a center line (CL) and upper and lower control limits (UCL and LCL in Figure 2.2). The center line represents where this process characteristic should fall if there are no unusual sources of variability present. The control limits are determined from some simple statistical considerations. Classically, control charts are applied to the output variable(s) in a system such as in Figure 2.2. However, in some cases they can be usefully applied to the inputs as well (Montgomery, 1997).

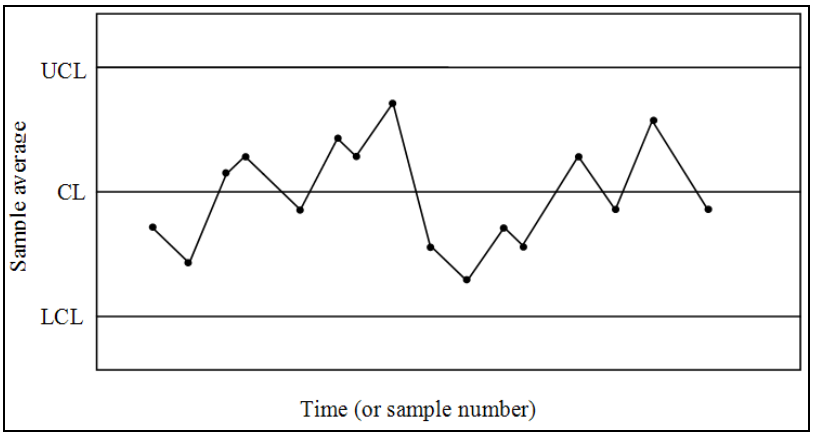

Figure 2.2 A typical control chart (Montgomery, 1997).

Stable systems are in a state of statistical control and exhibit only variability due to common causes. Control charts are based on the fact that change variation follows known patterns. These patterns are the statistical reference distributions such as the normal distribution (Levine, Ramsey, & Berenson, 1995). According to the normal distribution, the proportion area of normal distribution curve falls into segments defined by 1, 2, and 3 standard deviations from the mean. 99.73 percent of the area under a normal curve falls between plus and minus 3 standard deviations ($\pm 3\sigma$) from the mean (μ). This means only 0.0027 or 0.27 percent of the area lies beyond $\pm 3\sigma$ from the mean. If only change or common causes are operating, it is expected that to be beyond the range of $\pm 3\sigma$ range is only 0.0027. This is considered to be a

sufficient small probability for us to suspect that something other than change is operating and that a special cause may be present (Levine, Ramsey, & Berenson, 1995). Moreover, in many cases, the true distribution of the quality characteristic is not known well enough to compute exact probability limits. Some analysts suggest using two sets of limits on control charts. The outer limits, say at 3σ, are the usual *action limits*; that is, when a point plots outside of this limit, a search for an assignable cause is made and corrective action is taken necessary. The inner limits, usually at 2σ, are called *warning limits* (Montgomery, 1997).

There is a close connection between control charts and hypothesis testing. To illustrate this connection, suppose that the vertical axis in Figure 2.2 is the sample average $\bar{x}$. If the current value of $\bar{x}$ plots between the control limits, this means that the process mean is in-control; that is, it is equal to some value μ_0. On the other hand, if $\bar{x}$ exceeds either control limits, this means that the process mean is out-of-control; that is, it is equal to some value $\mu_1 \neq \mu_0$. In a sense, then the control chart is a test of the hypothesis that the process is in a state of statistical control. A point plotting within the control limits is equivalent to failing to reject the hypothesis of statistical control, and a point plotting outside the control limits is equivalent to rejecting the hypothesis of statistical control (Montgomery, 1997). In another words the aim of quality monitoring is to test the null hypothesis $H_0 : s = 0$ (in-control state of the process) against the alternative hypothesis $H_1 : s \neq 0$ (out-of-control state of the process) (Pacella & Semeraro, 2007), where *s* represents the mean shift. This hypothesis-testing framework is useful in many ways, but there are some differences in viewpoint between control charts and hypothesis tests. For example, when testing statistical hypothesis, the validity of assumptions are usually checked, while control charts are used to detect departures from an assumed state of statistical control. Furthermore, the assignable cause can result in many different types of shifts in the process parameters. For example, the mean could shift instantaneously to a new value and remain there (this is sometimes called a *sustained* shift); or it could shift abruptly but the assignable cause could be short lived and the mean could then return to its nominal or in-control value; or the assignable cause could result in a steady

drift or trend in the value of the mean. Only the sustained shift fits nicely within the usual statistical hypothesis testing model (Montgomery, 1997).

Specifying the control limits is one of the critical decisions that must be made in designing a control chart. By moving the control limits further from the center line, the risk of a type-I error is decreased - that is, the risk of a point falling beyond the control limits, indicating an out-of-control condition when no assignable cause is present. However, widening the control limits will also increase the risk of a type-II error - that is, the risk of a point falling between the control limits when the process is really out-of-control. If the control limits are moved closer to the center line, the opposite effect is obtained: the risk of type-I error is increased, while the risk of type-II error is decreased. It is occasionally helpful to use the operating characteristic curve of a control chart to display its probability of type-II error. This would be an indication of the ability of the control chart to detect process shifts of different magnitudes (Montgomery, 1997).

There are a wide variety of control charts that are developed to use in different processes. And also each of them has different characteristics and structure. So many different kinds of control charts developed from the first creation of the control chart and then they are improved to solve different kind of quality problems. The quality of a product can be evaluated using either an *attribute* of the product or a *variable* measure. An attribute is a product characteristic such as color, surface texture, or perhaps smell or taste. Attributes can be evaluated quickly with a discrete response such as good or bad, acceptable or not, or yes or no (Russell & Taylor, 1998). The types of control charts are classified into two groups. These include control charts for qualitative variables and control charts for quantitative variables measured at the interval or ratio level. Control charts such as those appropriate for characteristics measured as qualitative variables are referred to as *control charts for attributes*; and control charts such as those appropriate for characteristics measured on an interval or ratio scale of measurement are referred to as *control charts for variables.* Regression control charts (the control chart that we aim to modify it for autocorrelated data) are classified into the second classes that are *control charts for variables.* Each kind of

control chart has a corresponding method of determining the center line and control limits. Control charts such as those appropriate for characteristics measured as qualitative variables are referred to as control charts for attributes; in general they include control charts for (Tanya, 1999; Levine, Ramsey, & Berenson, 1995; Montgomery, 1997; Swift, Ross, & Omachonu, 1998):

1. Fraction nonconforming (p chart)
2. Number nonconforming (np chart)
3. Number of nonconformities (c chart)
4. Nonconformities per unit (u chart)
5. Demerits per unit (U chart)

Control charts such as those appropriate for characteristics measured on an interval or ratio scale of measurement are referred to as control charts for variables; for example they include:

1. Control chart for the mean ($\overline{x}$ chart)
2. Control chart for the standard deviation (*S* chart)
3. Control chart for the range (*R* chart)
4. Control chart for individual units (*x* chart)
5. Cumulative sum control chart for the process mean (CUSUM chart)
6. Exponentially weighted moving average control chart (EWMA chart)
7. Geometric moving average control chart (GMA)
8. Regression control chart
9. Modified control charts
10. Acceptance control chart
11. Hotelling's T^2 control chart and its variations

Each of these control charts has a corresponding method of determining the center line and control limits. SPC methods are usually applied in an environment when periodic sampling and rational subgrouping of process output is appropriate (Yourstone & Montgomery, 1989). Construction of a variable chart begins by

selecting samples or subgroups of process output for evaluation on a variables measure of a quality characteristic of interest. A measure of central tendency, such as the mean, and a measure of variability, such as the range or standard deviation are then calculated for each subgroup and these statistics are used to construct trial control limits. However, before begining to sample, several decisions must be made such as: sample size and frequency of sampling (Levine, Ramsey, & Berenson, 1995).

A *sample* is a subset of observations selected from a population (Montgomery & Runger, 1999). In designing a control chart, both the *sample size* to use and the *frequency of sampling* must be specified. In general, larger sample size will make it easier to detect small shifts in the process. When choosing the sample size, the size of the shift that we are trying to detect must be kept in mind. If the process shift is relatively large, then we use smaller sample sizes than those that would be employed if the shift of interest were relatively small (Montgomery, 1997). Also the frequency of sampling must be determined. The frequency with which samples are drawn is directly related to the control chart's ability to detect the precence of special causes or process shifts and inversely related to the time it takes to detect a shift once it occurs. In other words, the more frequently samples are drawn, the more sensitive the chart will be to the precence of special causes and the more quickly a shift in process average will be detected. The probability of detecting shifts quickly could be increased by using large sample sizes and sampling frequently. However, the practical constraints of most situations require us to balance sample size and frequency of sampling against budgetary requirements, time, and the costs of falling to detect a shift in the process (Levine, Ramsey, & Berenson, 1995). The most desirable situation from the point of view of detecting shifts would be to take large samples very frequently; however, this is usually not economically feasible. The general problem is one of *allocating sampling effort*. That is, either small samples at short intervals or larger samples at longer intervals are taken. Current industry practice tends to favor smaller, more frequent samples, particularly in high-volume manufacturing processes, or where a great many types of assignable causes can occur. Furthermore, as automatic sensing and measurement technology develops, it is

becoming possible to greatly reduce sampling frequencies. Ultimately, every unit can be tested as it is manufactured. Automatic measurement systems and microcomputers with statistical process control is an increasingly effective way to apply statistical process control (Montgomery, 1997).

A control chart may indicate an out-of-control condition either (i) when one or more points fall beyond the control limits or (ii) when the plotted points exhibit some nonrandom pattern of behavior. If the points are truly random, a more even distribution of them above and below the center line are expected. Also if following consecutive points in a row increase in magnitude is observed, this arrangement of points is called a *run*. Since the observations are increasing, this can be called as a run up. Similarly, a sequence of decreasing points is called a run down. This control chart has an unusually long run up and an unusually long run down. In general a run is defined as a sequence of observations of the same type. In addition to runs up and runs down, the types of observations are defined as those above and below the center line, respectively, so that two points in a row above the center line would be a run of length 2. A run of length 8 or more points has a very low probability of occurrence in a random sample of points. Consequently, any type of run of length 8 or more is often taken as a signal of an out-of-control condition. For example, eight consecutive points on one side of the center line will indicate that the process is out-of-control (Montgomery, 1997).

Figures 2.3b and 2.3c represent trends in the data and are characterized by the overall movement of points in one direction. Whenever observations in a sequence are the same type (for example, all increasing or all decreasing or all above the center line or all below the center line), that set of points is called a run. Figure 2.3b represents a run up (increasing trend), while Figure 2.3c represents a run down (decreasing trend). The special causes underlying these patterns include fatigue of personel or equipment, systematic environmental changes, buildup of waste products, or settling or separation in a chemical process (Levine, Ramsey, & Berenson, 1995).

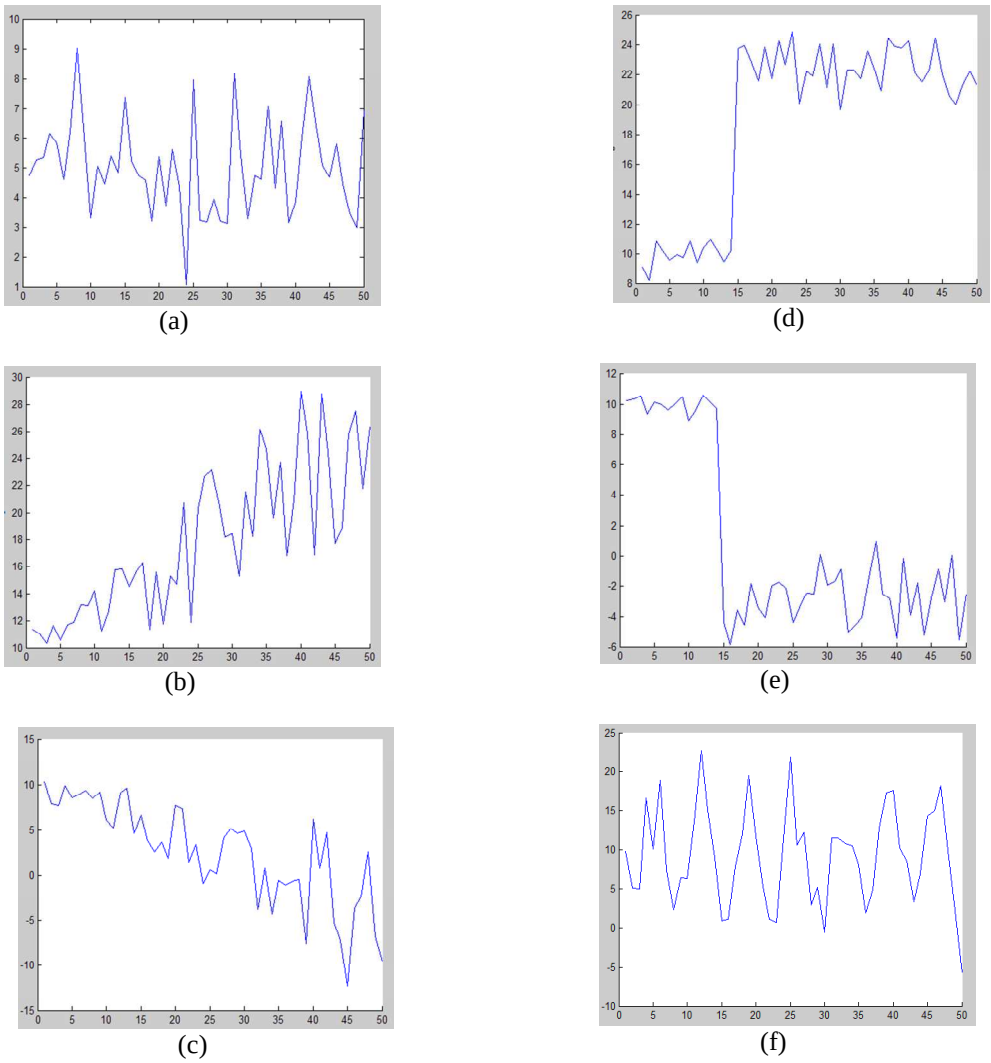

Figure 2.3 Typical patterns in control chart (a) Natural pattern, (b) Increasing trend pattern, (c) Decreasing trend pattern, (d) Upward shift pattern, (e) Downward shift pattern, (f) Cyclic pattern (Periodical shifting).

Control charts are among the most important management control tools; they are as important as cost controls and material controls. Modern computer technology has made it easy to implement control charts in any type of process, as data collection and analysis can be performed on a microcomputer or a local area network terminal in real-time, on-line at the work center. The performance of control charts are measured via *average run length* (ARL). Essentially, the ARL is the average number of points that must be plotted before a point indicates an out-of-control condition. ARL will be discussed in chapter four later.

As mentioned above, the fundamental assumption of the control charts is that the observations of the process are independent and identically distributed (iid). However, the independency assumption is not realistic in practice due to various reasons, and process observations become autocorrelated. In the next subsections the autocorrelation, time series and control charts for autocorrelated data will be examined, and regression and the conventional regression control chart will be discussed.

2.2 Autocorrelation and Time Series Models

The standard assumptions that are usually cited in justifying the use of control charts are that the data generated by the process when it is in-control are normally and independently distributed. Unfortunately, the assumption of uncorrelated or independent observations is not even approximately satisfied in some manufacturing processes. Examples include chemical processes where consecutive measurements on process or product characteristics are often highly correlated or automated test and inspection procedures, where every quality quality characteristic is measured on every unit in time order of production. Basically, all manufacturing processes are driven by internal elements, and when the interval between samples becomes small relative to these forces, the observations on the process will be correlated over time (Montgomery, 1997).

Autocorrelation is a state of having relationship between the consecutive observations. In another words, autocorrelation is the correlation of one variable a one point in time with observations of the same variable at prior time points. When there is significant autocorrelation in a process, traditional control charts will be ineffective because control charts are constructed under the assumption of using random observations which are independent and identically distributed. Within the framework of the Box-Jenkins methodology, time series models are characterized by their autocorrelation functions. The correlation between two random random variables, say W and Z, is defined as

$$\rho_{WZ} = \frac{Cov(W,Z)}{\sqrt{V(W)V(Z)}} \tag{2.1}$$

Thus the autocorrelation at lag *k* refers to the correlation between any two observations in a time series that are *k* period apart (Montgomery & Johnson, 1976). That is,

$$\rho_k = \frac{Cov(x_t, x_{t+k})}{\sqrt{V(x_t)V(x_{t+k})}} = \frac{\gamma_k}{\gamma_0} \tag{2.2}$$

is the autocorrelation at lag *k*, where γ_k is the autocovariance and γ_0 is the variance of autocorrelated process. A graphical display of ρ_k versus the lag *k* is called the autocorrelation function $\{\rho_k\}$ of the process. The autocorrelation function is dimensionless and that $-1 \leq \rho_k \leq 1$. Furthermore, $\rho_k = \rho_{-k}$ that is, the autocorrelation function is symmetric. So that it is necessary to consider only positive lags. In general, when observations *k* lags apart are close together in value, ρ_k is found close to 1.0. When a large observation at time *t* is followed by a small observation at time *t+k*, ρ_k is found close to -1.0. If there is little relationship between observations *k* lags apart, ρ_k is found approximately zero. Another useful concept in the description of time series models is partial correlation. Consider the three random variables *W, Y,* and *Z*. If the joint density function of *W, Y,* and *Z* be $f(W,Y,Z)$, then the conditional distribution of *W* and *Y* given *Z* is

$$h(W,Y|Z) = \frac{f(W,Y,Z)}{\int_{-\infty}^{\infty}\int_{-\infty}^{\infty} f(W,Y,Z)dWdY} \tag{2.3}$$

The correlation coefficient between *W* and *Y* in the conditional distribution $h(W,Y|Z)$ is called the partial (or conditional) correlation coefficient. That is the partial correlation between *W* and *Y* is just the simple correlation between *W* and *Y* with the effect of their correlation with Z removed. In terms of a time series, it is

convenient to think of the partial autocorrelation at lag *k* as the correlation between x_t and x_{t+k} with the effects of the intervening observations ($x_{t+1}, x_{t+2}, ..., x_{t+k-1}$) removed. Notationally, the *k* th partial autocorrelation coefficient shall be refered as ϕ_{kk}. A plot of ϕ_{kk} versus the lag *k* is called the partial autocorrelation function $\{\phi_{kk}\}$. It must be noted that $\phi_{kk} = \rho_0 = 1$ and $\phi_{11} = \rho_1$ (Montgomery & Johnson, 1976).

The matter of how to monitor an autocorrelated data has been discussed frequently in recent years. In order to use control charts effectively, the autocorrelation in the data must be removed. One method to remove the autocorrelation in the data is to fit the data to a time series model. A *time series* is a data set in which the observations are recorded in the order in which they occur (Box & Jenkins, 1976). In another words, a time series is a sequence of observations on a variable of interest. The variable is observed at discrete time points, usually equally spaced.

Time series analysis involves describing the process or phenomena that generate the sequence. A central feature in the development of time series models is an assumption of some form of statistical equilibrium. A particular assumption of this kind is that of stationarity. In analyzing a time series, it is regarded as a realization of a stochastic process. A very special class of stochastic processes, called stationary processes, is based on the assumption that the process is in a particular state of statistical equilibrium (Box & Jenkins, 1976). In stationary processes the mean and the variance of the measured values (x_t) must be constant (Mills, 1990). Stationary time series are modeled by autoregressive moving average (ARMA) models. Autoregressive model (AR(*p*) model) is a special case of ARMA models. The autoregressive process can be represented by the model given in Equation (2.4) (Box & Jenkins, 1976).

$$x_t = \xi + \phi_1 x_{t-1} + \phi_2 x_{t-2} + ... + \phi_p x_{t-p} + \varepsilon_t \qquad (2.4)$$

Equation (2.4) is called an autoregressive process because the current observation x_t is regressed on previous realizations $x_{t-1}, x_{t-2}, ..., x_{t-p}$ of the same time series. The process contains ρ unknown parameters $\phi_1, \phi_2, ..., \phi_p$ (apart from ξ and the unknown variance σ^2) and as a result Equation (2.4) is refered as an autoregressive process of order ρ, abbreviated AR(ρ). If $\rho = 1$ then Equation (2.4) becomes the first-order autoregressive or AR(1) process that is the representative model used in this thesis

$$x_t = \xi + \phi_1 x_{t-1} + \varepsilon_t \tag{2.5}$$

The AR(1) process is often called the Markow process because the observation at time t depends only on the observation at time $t-1$. We must have $|\phi_1| < 1$ for stationarity (Montgomery & Johnson, 1976; Box & Jenkins, 1976). The mean, variance and autocovariance of the AR(1) process are given, respectively in the following (Box & Jenkins, 1976):

$$\mu = E(x_t) = \frac{\xi}{1-\phi_1} \tag{2.6}$$

$$\gamma_0 = E(x_t - \mu)^2 = \frac{\sigma_\varepsilon^2}{1-\phi_1^2} \tag{2.7}$$

$$\gamma_k = E(x_t - E(x_t))(x_{t+k} - E(x_{t+k})) = \phi_1^k \frac{\sigma_\varepsilon^2}{1-\phi_1^2} \tag{2.8}$$

In an AR(1) model, the autocorrelation at lag *k* can be found easily from the Equations (2.7) and (2.8) (Box & Jenkins, 1976):

$$\rho_k = \frac{\gamma_k}{\gamma_0} = \phi_1^k \tag{2.9}$$

where $k \geq 0$.

2.3 Control Charts for Autocorrelated Processes

When there is significant autocorrelation in a process, traditional control charts with *iid* assumption can still be used, but they will be ineffective. When autocorrelation is presented, there are problems of noticing “special causes” that do not exist and not detecting “special causes” that truly exist, implying a high probability of false positives and / or false negatives (Eleni, Demetrios, & Leonidas, 2005). In other words these charts will results poor ARL performance like high false alarm rates and slow detection of process shifts (Zhang, 2000). Because of this reason some modifications for traditional control charts are necessary if autocorrelation cannot be ignored. Therefore, various control charts have been developed for monitoring autocorrelated processes.

A common approach to detect a possible process mean shift in the autocorrelated data is to use residual control charts, also known as the special cause chart (SCC), which are constructed by applying traditional SPC charts (Shewhart, CUSUM, EWMA and etc.) to the residuals from a time series model of the process data (Zhang, 2000). In these charts, forecast errors, namely residuals, are assumed to be statistically uncorrelated. An appropriate time series model is fitted to the autocorrelated data and the residuals are plotted in a control chart. For this reason all of the well-known control schemes can be transformed to the residual control scheme.

In this study, we made a comprehensive review and observed that different charting techniques for residuals were developed to accommodate autocorrelated data. Alwan & Roberts (1988) introduced the common cause chart (CCC) which is applied by forming an ARIMA model for the autocorrelated process. CCC is not a control chart actually, because it does not have any control limits. It consists of only plotted data which have been modeled with an ARIMA model. The CCC is a plot of the fitted values or forecasts obtained when data are fitted with appropriate time series model. It was intended to give a representation of the predicted state of the quality characteristic without any control limits (Samanta & Bhattacherjee, 2001).

Furthermore, Alwan & Roberts (1988) developed a residual Shewhart chart and called it the special cause chart (SCC). The basic idea in the SCC method is to transform the original autocorrelated data to a set of "residuals" and monitor the residuals. Shewhart, CUSUM or EWMA control charts are the most frequently used control charts for residuals.

Shewhart chart, firstly introduced by Dr. Walter A. Shewhart (1931), attracted many scientists' interest. Since the first statistical control charts $\bar{x}$, $\bar{x}$ and R, $\bar{x}$ and S, were introduced by Shewhart, these charts are called the Shewhart control charts. The Shewhart $\bar{x}$ and R chart which is the basis for many control charts is very simple and easy to use. If x_t are sample of size *n*, then the average of this sample is $\bar{x}$ and it is well known that $\bar{x}$ is normally distributed with mean μ and standard deviation $\sigma_{\bar{x}}$, where $\sigma_{\bar{x}} = \sigma / \sqrt{n}$. Then the best estimator of μ, the process average, is the grand average, say $\bar{\bar{x}}$. Then the center line (CL), upper control limit (UCL), and lower control limit (LCL) of the chart for the 3 standard deviations from the centerline are given below in Equation (2.10-2.12) respectively (Montgomery, 1997; Oakland, 2003):

$$UCL = \bar{\bar{x}} + 3\frac{\sigma}{\sqrt{n}} \tag{2.10}$$

$$CL = \bar{\bar{x}} \tag{2.11}$$

$$LCL = \bar{\bar{x}} - 3\frac{\sigma}{\sqrt{n}} \tag{2.12}$$

where $\bar{\bar{x}} = (\bar{x}_1 + \bar{x}_2 + ... + \bar{x}_m)/m$, $\bar{x} = (x_1 + x_2 + ... + x_n)/n$, $\hat{\sigma} = \bar{R}/d_2$, $R = x_{\max} - x_{\min}$ and $\bar{R} = (R_1 + R_2 + ... + R_m)/m$. If the production rate is too slow to allow sample sizes greater than one then individual measurements are used. For the control chart for individual measurements, the parameters are

$$UCL = \bar{x} + 3\frac{\overline{MR}}{d_2} \tag{2.13}$$

$$CL = \bar{x} \tag{2.14}$$

$$LCL = \bar{x} - 3\frac{\overline{MR}}{d_2} \tag{2.15}$$

where $\overline{MR}$ is the moving range and MR is the range between consecutive observations. If the observations are autocorrelated, the formulations are modified by using $\{e_t\}$ instead of $\{x_t\}$. For residual charts, the residual e_t from a time series model of $\{x_t\}$ is defined as

$$e_t = x_t - \hat{x}_t \tag{2.16}$$

where $\hat{x}_t$ is the prediction of $\{x_t\}$ from the time series model at time *t*. Various residual charts are constructed based on e_t depending on the traditional charts used. For a Shewhart residual chart, the chart is constructed by charting e_t instead of $\{x_t\}$. Also the other residual control charts such as CUSUM residual, EWMA residual and GMA residual charts are constructed by applying traditional CUSUM, EWMA and GMA charts respectively to $\{e_t\}$ (Zhang 2000; Montgomery, 1997; Montgomery & Runger, 1999; Montgomery & Johnson, 1976). $\bar{e}_t$ is the centerline of the Shewhart residual control chart. If the least squares regression is used to fit the relationship between *x* and *y*, then $\bar{e}_t$=0. The $3\hat{\sigma}_e$ control limits are used for the shewhart cause selecting chart where $\sigma_{\bar{e}}$ is the standard deviation of the process errors (Shu & Tsung, 2000). e_t shows normal distribution with mean zero and with constant variance. Now, conventional Shewart control chart can be applied to residuals.

Shewhart control charts have been used in practice for decades because they do not need deep statistical knowledge and they are easy to use and interpret. Beside these advantages, Shewhart charts have also some disadvantages. The first drawback is, it takes much longer for a Shewhart chart to detect the mean shift. The second drawback of a Shewhart control chart is that, crucial issue of any Shewhart control chart is that it only takes into consideration the last plotted point, and can not contain information about the whole process. In another words these charts typically do not take into account previous data points, except in the case of using run rules. Because of this feature, Shewhart charts are usually effective for detecting large shifts but ineffective for detecting small shifts (about 1.5 or less) in process parameters. An important shortcoming for Shewhart charts is to be ineffective for detecting small shifts. To overcome this disadvantage two different control charts, CUSUM and EWMA, are proposed (Montgomery, 1997). They are appropriate for detecting small shifts, because they give smaller weight to the past data. A CUSUM chart is able to look at historic data to determine if the data trend shows a shift in the data. The CUSUM chart is widely used to monitor the mean of a process. It is better than the standard Shewhart chart in that it is able to detect small deviations from the mean (Kudo, 2001). By the choice of weighting factor, λ (also known as 'smoothing constant'), the EWMA control procedure can be made sensitive to a small or gradual drift in the process. However, they do not react to large shifts as quickly as the Shewhart chart.

The CUSUM chart was firstly introduced by Page in 1954. The basic purpose of a CUSUM chart is to track the distance between the actual data point and the grand mean. Then, by keeping a cumulative sum of these distances, a change in the process mean can be determined, as this sum will continue getting larger or smaller. These cumulative sum statistics are called the upper cumulative sum (C_t^+) and the lower cumulative sum (C_t^-). They are defined by Equation (2.17) and Equation (2.18):

$$C_t^+ = \max[0, x_t - (\mu_0 + K) + C_{t-1}^+] \tag{2.17}$$

$$C_t^- = \max[0, (\mu_0 - K) - x_t + C_{t-1}^-] \quad (2.18)$$

where μ_0 is the grand mean and *K* is the slack value which is often chosen about halfway between the target μ_0 and the out-of-control value of the mean μ_1 that we are interested in detecting quickly (Montgomery, 1997; Oakland, 2003; Wetherill & Brown, 1991). So, if the shift is expressed in standard deviation units as $\mu_1 = \mu_0 + \delta\sigma$ (or $\delta = |\mu_1 - \mu_0| / \sigma$), then *K* is one-half the magnitude of the shift or $K = (\delta\sigma)/2 = (|\mu_1 - \mu_0|)/2$. It is important to select the right value for *K*, since a large value of *K* will allow for large shifts in the mean without detection, whereas a small value of *K* will increase the frequency of false alarms. Normally, *K* is selected to be equal to 0.5σ.

The tabular CUSUM is designed by choosing values for the reference value *K* and the decision interval *H*. Define $K = k\sigma$ and $H = h\sigma$, where σ is the standard deviation of the sample variable used in forming the CUSUM. Using *h*=4 or *h*=5 and *k*=1/2 will generally provide a CUSUM that has good ARL properties against a shift about 1σ in the process mean (Montgomery, 1997). For CUSUM residual chart, the residuals are calculated using Equation (2.16) where e_t shows normal distribution with mean zero and with constant variance. Then, conventional CUSUM control chart can be applied to the residuals using the formulas given in Equation (2.17) and Equation (2.18). CUSUM control chart is especially effective with processes whose sample sizes are one (*n*=1). Due to this feature of CUSUM control chart, it is effectively used in individual observations one such as chemical and process industries, and discrete parts manufacturing with automatic measurement of each part.

The EWMA chart was proposed by Roberts in 1959. Like CUSUM chart, EWMA is suitable for detecting small process shifts. EWMA chart uses smoothing constant where the smoothing constant λ is that $0 < \lambda \leq 1$ (Shu, Tsung, & Tsui, 2005). The EWMA is a statistic for monitoring the process that averages the data in a way that gives less and less weight to data as they are further removed in time. By the

choice of weighting factor λ, the EWMA control procedure can be made sensitive to a small or gradual drift in the process. The statistic that is calculated is (Montgomery, 1997):

$$z_t = \lambda x_t + (1-\lambda) z_{t-1} \tag{2.19}$$

where z_t is the moving average at time *t*. The value of λ can be between zero and one, but it must often chosen between 0.05 and 0.3. The initial value of *z* (i.e. z_0) is set to the grand mean (μ_0) (Montgomery, 1997; Oakland, 2003; Wetherill & Brown, 1991). If the observations x_t are independent random variables with variance σ^2, then the variance of z_t will be

$$\sigma_{z_t}^2 = \sigma^2 \left(\frac{\lambda}{2-\lambda} \right) \left[1-(1-\lambda)^{2t} \right] \tag{2.20}$$

Therefore the EWMA control chart would be constructed by plotting z_t versus the time *t* (or sample number). The center line and control limits for the EWMA control chart are as follows:

$$UCL = \mu_0 + L\sigma \sqrt{\frac{\lambda}{(2-\lambda)} [1-(1-\lambda)^{2t}]} \tag{2.21}$$

$$CL = \mu_0 \tag{2.22}$$

$$LCL = \mu_0 - L\sigma \sqrt{\frac{\lambda}{(2-\lambda)} [1-(1-\lambda)^{2t}]} \tag{2.23}$$

where *L* is the number of standard deviations from the centerline (width of the control limits). Choise of weight factor is another problem. The parameter λ determines the rate at which 'older' data enter into the calculation of the EWMA statistic. A value of $\lambda = 1$ implies that only the most recent measurement influences

the EWMA (degrades to Shewhart chart). Thus, a large value of $\lambda = 1$ gives more weight to recent data and less weight to older data; a small value of λ gives more weight to older data. The value of λ is usually set between 0.2 and 0.3 although this choice is somewhat arbitrary. Lucas & Saccucci (1990) give tables that help the user to select λ. The term $[1-(1-\lambda)^{2t}]$ in Equation (2.21) and Equation (2.23) approaches unity as *t* gets larger. This means that after the EWMA control chart has been running for several time periods, the control limits will approach steady-state values given by (Montgomery, 1997)

$$UCL = \mu_0 + L\sigma\sqrt{\frac{\lambda}{(2-\lambda)}} \tag{2.24}$$

$$LCL = \mu_0 - L\sigma\sqrt{\frac{\lambda}{(2-\lambda)}} \tag{2.25}$$

However, in the literature, it is strongly recommend using the exact control limits in Equation (2.21) and (2.23) for small values of *t*. This will greatly improve the performance of the control chart in detecting an off-target process immediately after the EWMA is started up (Montgomery, 1997). For EWMA residual chart, the residuals are calculated using Equation (2.16) and then, conventional EWMA control chart can be applied to the residuals using the formula given in Equation (2.19). The EWMA is a statistic for monitoring the process that averages the data in a way that gives less and less weight to data as they are further removed in time. CUSUM and EWMA are appropriate for detecting small shifts, because they give smaller weight to the past data. However, they do not react to large shifts as quickly as the Shewhart chart.

Another residual charts, geometric moving average (GMA) and geometric moving range (GMR) control charts were studied by Yourstone & Montgomery (1989). The geometric moving range between successive pairs of residuals is used to track the dispersion of the process quality data in the real-time SPC algorithm. The geometric moving range allows the user of the algorithm to alter the sensitivity of the

moving range filter through adjustments to the smoothing constant. Two years later, in 1991, they proposed two innovative control charts, the sample autocorrelation chart (SACC) and the group autocorrelation chart (GACC) which are shown to be particularly effective control schemes when used control chart for the residuals of the time series model of the real time process data. These charts are based on the autocorrelation function of autocorrelated data. The SACC as well as the GACC detect shifts in the mean as well as shifts in the autocorrelative structure. The GACC chart detects the shift before the SACC since the GACC detects fluctuations over all lags of the sample autocorrelation. The SACC will signal shifts through a change in the pattern of the plots of the sample autocorrelation as well as through plots meeting or exceeding the control limits. The GACC will detect shifts that impact the sample autocorrelations as a group (Yourstone & Montgomery, 1991). When compared with the previous methods, SACC is less sensitive in detecting mean and variance shifts but very competitive in detecting changes in the parameters of ARMA model (Atienza, Tang, & Ang, 1997).

Today, many industrial products are produced by several dependent process steps not just one step. However, conventional SPC techniques focus mostly on individual stages in a process and do not consider disseminating information throughout the multiple stages of the process. They are shown to be ineffective in analyzing multistage processes. A different approach to this problem is the cause-selecting chart (CSC), proposed by Zhang (1984). The CSC based on the output adjusted for the effect of the incoming quality shows promise for increasing the ability to analyze multistage processes (Yang & Yang, 2006).

On the other hand, the traditional practice in using the control charts to monitor a process is to use a fixed sampling rate (FSR) which takes samples of fixed sample size (FSS) with a fixed sampling interval (FSI). In recent years, several modifications adopting the variable sampling interval (VSI), variable sample size (VSS) and variable sampling rate (VSR) or variable sampling interval and sampling size (VSSI) in the $\bar{x}$ control chart have been suggested to improve traditional FSI policy and have been shown to give better performance than the conventional $\bar{x}$ charts in the

sense of quick response to process change in the quality control literature. The VSSI features are extended to CUSUM and EWMA charts. Zou, Wang, & Tsung (2008) suggested using a variable sampling scheme at fixed times (VSIFT) to enhance the efficiency of the $\bar{x}$ control chart for the autocorrelated data. Two charts are under consideration, that is, the VSIFT $\bar{x}$ chart and variable sampling rate with sampling at fixed times VSRFT $\bar{x}$ charts. These two charts are called $\bar{x}$-VSFT charts.

Traditional residual based charts, such as a Shewhart, CUSUM, or EWMA on the residuals, do not make use of the information contained in the dynamics of the fault signature. In contrast, methods such as the cumulative score (Cuscore) charts which are presented by Box & Ramirez (1992) or generalized likelihood ratio test (GLRT) do incorporate this information. Traditional control charts are intended to be used in high volume manufacturing. In a short run situation, there is not enough data available for the estimation purposes. In processes where the length of the production run is short, data to estimate the process parameters and control limits may not be available prior to the start of production, and because of the short run time, traditional methods for establishing control charts cannot be easily applied. Many sampling difficulties arise when applying standard control charts in low volume manufacturing horizon. *Q* charts have been proposed to address this problem by Quesenberry (1991) (Castillo & Montgomery, 1994).

The basic idea in the SCC method is to transform the original, autocorrelated data to a set of "residuals" and monitor the residuals. The minimum mean squared error (MMSE) predictor used in the SCC chart is optimal for reducing the variance of the residuals but is not necessarily best for the purposes of process monitoring. Furthermore, the MMSE predictor is closely tied to a corresponding MMSE scheme in feedback control problems. Despite a huge literature on MMSE-based feedback control, the class of proportional integral derivative (PID) control schemes is more common in industry (see Box, Jenkins, & Reinsel (1994); Astrom & Hagglund (1995) refered from (Jiang, Wu, Tsung, Nair, & Tsui, 2002)). Jiang et al. (2002) used an analogous relationship between PID control and the corresponding PID predictor to propose a new class of procedures for process monitoring. As in SCC charts, they

transformed the autocorrelated data to a set of "residuals" by subtracting the PID predictor and monitoring the residuals.

When the literature is reviewed for 1997-2010 year range, it is clearly observed that the following studies are remarkable for residual control charts. After reviewing residual control charts, the review for modified control charts will be presented in the consequent paragraphs. Kramer & Schmid (1997) discussed the application of the Shewhart chart to residuals of AR(1) process and in the same year Reynolds & Lu (1997) compared performances of two different types of EWMA control charts for residuals of AR(1) process. Yang & Makis (1997) compared the performances of Shewhart, CUSUM, EWMA charts for the residuals of AR(1) process. Zhang (1997) remarked that the detection capability of an *x* residual chart was poor for small mean shifts compared to the traditional *x* chart, EWMA, and CUSUM charts for AR(2) process. Two years Lu & Reynolds (1999) compared the performances of EWMA control chart based on the residuals from the forecast values of AR(1) process and EWMA control chart based on the original observations. Luceno & Box (2000) studied the One-sided CUSUM chart. Rao, Disney & Pignatiello (2001) focused on the integral equation approach for computing the ARL for CUSUM control charts for AR(1) process. They studied the ARL performance versus length of the sampling interval between consecutive observations for residuals of AR(1) process. Jiang et al. (2002) proposed proportional integral derivative (PID) charts for residuals of ARMA(1,1) process. Kacker & Zhang (2002) studied the run length performance of Shewhart $\bar{x}$ for residuals of IMA(λ, σ) processes. Shu, Apley, & Tsung (2002) proposed a CUSUM-triggered Cuscore chart to reduce the mismatch between the detector and fault signature. A variation to the CUSUM-triggered Cuscore chart that uses a GLRT to estimate the mean shift time of occurrence is also discussed. They used ARMA(1,1) process to test the performance of proposed chart. It is shown that the triggered Cuscore chart performs better than the standard Cuscore chart and the residual-based CUSUM chart. Ben-Gal Morag, & Shmilovici (2003) presented context-based SPC (CSPC) methodology for state-dependent discrete-valued data generated by a finite memory source and tested the performance of this new modified chart for AR(1), AR(2), MA(1) processes. Snoussi, Ghourabi, & Limam (2005)

studied on residuals for short run autocorrelated data of autocorrelated process. They compared the performances of Shewhart $\bar{x}$, CUSUM, and EWMA control charts for residuals of AR(1) process. They also compared the performances of CUSUM, and EWMA control charts with Q statistics (EWMA Q chart and CUSUM Q chart) for residuals of AR(1) process. Kim, Alexopoulos, Goldsman, & Tsui (2006) considered a CUSUM process as their monitoring statistic that is a bit different than that of Johnson & Bagshaw (1974), and they approximate this CUSUM process by a Brownian motion process. Noorossana & Vaghefi (2006) investigated the effect of autocorrelation on performance of the MCUSUM control chart. Triantafyllopoulos (2006) has developed a new multivariate control chart based on Bayes' factors. This control chart is specifically aimed at multivariate autocorrelated and serially correlated processes and tested for AR(1) process. Yang & Yang (2006) considered the problem of monitoring the mean of a quality characteristic *x* on the first process step and the mean of a quality characteristic *y* on the second process step, in which the observations *x* can be modeled as an AR(1) model and observations *y* can be modeled as a transfer function of *x* since the state of the second process step is dependent on the state of the first process step. To effectively distinguish and maintain the state of the two dependent process steps, the Shewhart control chart of residual and the cause selecting chart (CSC) are proposed. They showed that the proposed control charts are much better than the misused Hotelling T^2 control chart and the individual shewhart chart. Ghourabi & Limam (2007) proposed a new method of residual process control, the Pattern Chart and tested this new chart for AR(1) process and compared its ARL values with SCC chart. Costa & Claro (2008) considered the double sampling (DS) $\bar{x}$ control chart for monitoring processes in which the observations can be represented as ARMA(1,1) model. Zou, wang, & Tsung (2008) suggested using a variable sampling scheme at fixed times (VSIFT) to enhance the efficiency of the $\bar{x}$ control chart for the autocorrelated data. Two charts are under consideration, that is, the VSIFT $\bar{x}$ and variable sampling rate with sampling at fixed times (VSRFT $\bar{x}$) charts. These two charts are called $\bar{x}$-VSFT charts. The authors used AR(1) model as representative model for their study. An integration equation method combined with a Markov process model was developed to study the performance of these charts. Sheu & Lu (2009) examined a GWMA with

a time-varying control chart for monitoring the mean of a process based on AR(1) process and they compared ARL performance of GWMA and EWMA charts. Weiss & Testik (2009) investigated the CUSUM control chart for monitoring autocorrelated processes of counts modeled by a Poisson integer-valued autoregressive model of order 1 (Poisson INAR(1)). Knoth, Morais, Pacheco, & Schmid (2009) discussed the impact of autocorrelation on the probability of misleading signals (PMS) of simultaneous Shewhart and EWMA residual schemes for the mean and variance of a AR(1) process. Lu & Ho (2010) compared the ARL performance of various GWMA control charts between observations and residuals to consider how ARL differ in each case.

The main advantage of a residual chart is that it can be applied to any autocorrelated data whether the process is stationary or not. Residual control charts are the ease of interpretation and straightforward implementation that requires only a least-squares regression computer program to process the data prior to constructing the control charts (Zhang, 2000). Although the residual charts have some advantages by using them for autocorrelated processes, there are some problems. One of the most important disadvantages of residual charts is that the time series modeling knowledge is needed for constructing the ARIMA model and some residual charts which based on two valid time series models signal differently. The another problem is due to the detection capability of the residual chart. Harris & Ross (1991) recognized that the CUSUM control chart and EWMA control chart for the residuals from a first-order autoregressive (AR(1)) process may have poor capability to detect the process mean shift. Wardell, Moskowitz, & Plante (1994) showed that Shewhart charts are not completely robust to deviations from the assumption of process randomness; namely when observations are correlated. EWMA chart is very good at detecting small shifts, and performs well for large shifts at only the case when the autoregressive parameter is negative and the moving average parameter is positive. No other chart is obviously dominant under every condition. They showed that when the processes were positively autocorrelated (at the first lag), the residual chart did not perform very well. Zhang (1997) also studied on detection capability of residual chart for autocorrelated data. In his study, Zhang defined a measure of the detection

capability of the residual *x*-chart for the general stationary process and showed that the detection capability of a residual chart for AR(2) process was small compared to the detection capability of the *x* chart (Zhang, 1998). The detection capability of a Shewhart residual chart is smaller than the traditional Shewhart chart and other residual charts, EWMA and CUSUM residual charts (Harris & Ross, 1991; Longnecker & Ryan, 1992; Wardell, Moskowitz, & Plante, 1994; Zhang, 1998).

To overcome the disadvantages of residual-based control charts, monitoring the autocorrelated observations by modifying the standard control limits to account for the autocorrelation is suggested. This second approach, modified control chart, is based on applying the original control chart methodology with a little modification. Autocorrelated data is used in original control chart by adjusting its control limits. Control charts such as MCEWMA, EWMAST, and ARMA that are proposed for autocorrelated process observations are introduced to deal with the disadvantages of the residual charts and effectively used for stationary autocorrelated process data. Since rearrangement of the control limits for autocorrelated data is not so easy, application of modified charts is more complicated then the first approach.

MCEWMA control chart is used for individual observations and proposed by Montgomery and Mastrangelo in 1991. The MCEWMA chart is based on the familiar EWMA chart that is also standard in the literature; however, it adapts the EWMA for the autocorrelated data given by the ARIMA disturbance model (Nembhard, Mastrangelo, & Kao, 2001). Montgomery & Mastrangelo (1991) point out that it is possible to combine information about the state of statistical control and process dynamics on a single control chart. EWMAST control chart has been introduced by Zhang in 1998 to deal with the disadvantages of the residual charts. EWMAST chart is an extension of the traditional EWMA chart and basically constructed by charting the EWMA statistics for stationary process. EWMAST chart is a EWMA chart for stationary processes. Zhang (1998) remarked that the limits of the EWMAST chart are different from that of the traditional EWMA chart when the data are autocorrelated. When the process is positively autocorrelated, the limits of the EWMAST chart are wider than that of the ordinary EWMA chart. Zhang showed

that a EWMA of a stationary process is asymptotically a stationary process. The autocovariance function of EWMA is derived when the process is stationary. Then the EWMAST chart for general stationary process is established. The control limits of the EWMAST chart are analytically determined by the process variance and autocorrelation. When the process is nonstationary or near nonstationary with strong and positive autocorrelations, residual charts can be used. When the mean shifts are small, however, the performance of the residual chart is still satisfactory. Actually, no process control chart performs well in this case. In general, nonstationarity or near nonstationarity with positive autocorrelation is likely to occur when the data are acquired at high frequency. In this case the large in-control ARLs (such as those of the EWMAST chart) are often desirable, and the corresponding large out-of-control ARLs are much less a problem (Zhang, 1998). SCC chart is shown to be effective when detecting large shifts. The EWMAST chart performs better than the SCC chart when the process autocorrelation is not very strong and the mean changes are not large. On the other hand, the EWMAST chart applies the EWMA statistic directly to the autocorrelated process without identifying the process parameters and shown to be efficient in some parameter regions (Jiang, Tsui, & Woodal, 2000). An obvious advantage of using EWMAST chart is that there is no need to build a time series model. The EWMAST chart is easy to implement just like its special case, ordinary EWMA chart. On the other hand, implementation of a residual chart needs a time series modeling algorithm (Zhang, 1998).

By integrating the advantages of SCC chart and EWMAST chart and taking into account the autocorrelation structure of the underlying process, a family of control charts, the ARMA chart is proposed by Jiang, Tsiu, & Woodal (2000). This charting technique based on an autoregressive moving average (ARMA) statistic and provides a more flexible choise of parameters to relate the autocorrelation structure of the statistic to the chart performance and includes the special cause chart (SCC) chart and the EWMAST chart as special cases. It is shown that an ARMA chart with appropriate parameter values will outperform both the SCC and EWMAST charts for autocorrelated processes. Jiang et al. (2000) use the same notation of the EWMAST

chart proposed by Zhang (1998), and denote the ARMA chart as the ARMAST chart that is proposed for stationary processes.

On the other hand, the limitations of distribution-based procedures can be overcome by distribution-free SPC charts. Runger & Willemain (R&W) (1995) organized the sequence of observations of the monitored process into adjacent nonoverlapping batches of equal size; and their SPC procedure called unweighted batch means (UBM) is applied to the corresponding sequence of batch means. They choose a batch size larger enough to ensure that the batch means are approximately iid normal, and then they apply to the batch means one of the classical SPC charts developed for iid normal data, including the Shewhart and tabular CUSUM charts. In contrast to this approach, Johnson & Bagshaw (J&B) (1974) and Kim, Alexopoulos, Goldsman, & Tsui (2006) presented CUSUM based methods that use raw (unbatched) observations instead of batch means. Computing the control limits for the latter two procedures requires an estimate of the variance parameter of the monitored process that is the sum of covariances at all lags (see Kim et al. (2006) for experimental evaluations of R&W chart and J&B chart).

Kim et al. (2006) considered a CUSUM process as their monitoring statistic that is a bit different than that of Johnson & Bagshaw (1974), and they approximate this CUSUM process by a Brownian motion process. By exploiting the known properties of Brownian motion, they derive a new model-free CUSUM chart called the MFC Chart. The proposed SPC procedure requires the asymptotic variance constant which is the sum of covariances of all lags, the procedure is completely model-free - including the design of control limits and chart parameters - with the help of non-parametric variance estimation techniques popular in the simulation community. The MFC chart can be used with raw observations or batch means of any size, so using large batches can be avoided. Also this procedure provides a convenient way to compute control limits like the Shewhart chart does (Kim et al., 2006). Another distribution-free chart is run sum chart proposed by Willemain & Runger (1998) (Willemain & Runger, 1998). Their use of run sums is revival of an earlier idea. The use of coded run sums for iid data was described by Roberts (1996), who cited earlier

work by Toda (1958), who in turn cited Imaizuma (1955) and Reynolds (1971) presented a simplified overview (Willemain & Runger, 1998). The run sum chart proposed by Willemain & Runger (1998) differs from these earlier works in two significant ways. First, they consider the autocorrelated data characteristic of data-rich environments. Second, they use the sums of the observations directly, whereas earlier work coded the data values into integer scores before summing. Most SPC methods are not suitable for monitoring nonlinear and state-dependent processes. Another approach to developing distribution-free SPC charts is taken by Ben-Gal, Morag, & Shmilovici (2003). They presented context-based SPC (CSPC) methodology for state-dependent discrete-valued data generated by a finite memory source. The key idea of the CSPC is to monitor the statistical attributes of a process by comparing two context trees at any monitoring period of time. The first is a reference tree that represents the "in-control" reference behavior of the process; the second is a monitored tree, generated periodically from a sample of sequenced observations that represents the behavior of the process at that period. The Kullback–Leibler (KL) statistic is used to measure the relative "distance" between these two trees, and an analytic distribution of this statistic is derived. Monitoring the KL statistic indicates whether there has been any significant change in the process that requires intervention. The proposed CSPC extends the scope of conventional SPC methods. It allows the operators to monitor varying-length state-dependent processes as well as independent and linear ones. The CSPC is more generic and less model-biased with respect to time series modeling. The major drawback of CSPC is relatively large sample size required during the monitoring stage. Therefore, it should be applied primarily to processes with high sampling frequency, such as the buffer-level monitoring process. The CSPC is currently limited to discrete and single-dimensional processes (Ben-Gal, Morag, & Shmilovici, 2003). For distribution free processes "distribution free charts" are suggested. Kim, Alexopoulos, Tsui, & Wilson (2007) proposed a distribution free tabular CUSUM (DFTC) chart to detect mean shifts of autocorrelated observations. The authors defined the proposed chart as "a generalization of the conventional tabular CUSUM chart that is designed for iid normal random variables".

The following studies are remakable for modified control charts for autocorrelated data. As refered before, Zhang (1998) proposed EWMAST control chart, which is a modified control chart for autocorrelated data, and tested this new chart for AR(1), AR(2), ARMA(1,1) processes. Willemain & Runger (1998) proposed run sum chart which is a distribution-free chart and examined the residuals of AR(1) and ARMA(1,1) processes. Apley & Shi (1999) presented an on-line SPC technique, based on a GLRT, for detecting and estimating mean shifts in autocorrelated processes that follows a normally distributed ARIMA(4,0,3) model. The GLRT is applied to the uncorrelated residuals of the appropriate time-series model. The performance of GLRT is compared to Shewhart and CUSUM charts. By integrating the advantages of SCC chart and EWMAST chart and taking into account the autocorrelation structure of the underlying process, a family of control charts, the ARMA chart is proposed by Jiang, Tsiu, & Woodal (2000). They compared the performances of ARMA, ARMAST, EWMAST, EWMA, CUSUM and Shewhart control charts for AR(1), ARMA(1,1) processes. Later in (2001) jiang performed the average run length computation of ARMA charts for stationary processes and developed a Markow chain model for evaluating the run length performance of the ARMA chart applied to an ARMA (p,q) process. By exploiting the known properties of Brownian motion, they derive a new model-free CUSUM chart called the MFC Chart and tested this new chart for AR(1) process. Winkel & Zhang (2004) compared the performances of EWMA for the residuals of AR(1) process and EWMAST control charts for AR(1) process. Brence & Mastrangelo (2006) explored the capabilities of the tracking signals and the MCEWMA when the smoothing constants are varied and a shift is introduced into the AR(1) and ARMA(1,1) processes. Kim et al. (2007) proposed a distribution free tabular CUSUM (DFTC) chart to detect mean shifts in autocorrelated and normal distributed process observations. Stationary AR(1) and AR(2) processes are used to test its performance. Cheng & Chou (2008) used ARMA control chart in a real-time inventory decision system using Western Electric run rules. They monitored the data of demand that presents a pattern of time series. They employed ARMA chart to monitor the market demand that is autocorrelated and used individual control chart to monitor the inventory level. Issam & Mohamed (2008) proposed to apply support vector regression (SVR) method for

construction of a residual multivariate CUSUM (MCUSUM) chart, for monitoring changes in the process mean vector. Koksal, Kantar, Ula, & Testik (2008) investigated the effect of Phase I sample size on the run length performance of Residual chart, modified Shewhart chart, EWMAST chart and ARMA chart for monitoring the changes in the mean of AR(1) process.

In recent years, researchers have been investigating the use of artificial neural networks (NNs) in the application of control chart pattern (CCP) recognition with encouraging results. A neural network is an approach to data processing that does not require model or rule development. When compared to other methodologies the neural network approach has certain advantages. The model development is much simpler than that for most other approaches. Instead of theoretical analysis and development for a new model, the neural network tailors itself to the training data. The model can be refined at any time with the addition of new training data (Cheng, 1997). Also note that, a traditional control chart considers only the current sample when determining the status of a process and hence does not provide any pattern related information. NN based process control charts can classify patterns that the traditional charting methods for autocorrelated data cannot properly handle (Guh, 2008). Because of these advantages application of NNs to SPC has great interest in recent years. Although there are some disadvantages such as training requires considerable computation and training of these NNs will require many datasets; the recall process is very fast (Cheng, 1997). The application of NNs to SPC can be commonly classified into two categories: (i) control chart pattern recognition and (ii) detection of unnatural behavior (Pacella & Semeraro, 2007). In the second category, NN used to diagnose the shift in the mean of a manufacturing process.

Few studies on mean shift detection of autocorrelated processes by a neural-based approach were presented. West, Mangiameli, & Chen (1999) investigated the ability of radial basis function NNs to monitor and control complex manufacturing processes that exhibit both auto and cross-correlation. They demonstrated that the radial basis function network is superior to three control models proposed for complex manufacturing processes: multivariate Shewhart, MEWMA, and a feed

forward NN with logistic units trained by backpropagation (often called a back propagation neural network (BPN)). They used vector AR(1) (VAR(1)) model as the representative process model for their work. Chiu, Chen, & Lee (2001) used BPN to identify shifts in process parameter values from AR(1) process. Pacella & Semeraro (2007) proposed Elman recurrent neural network for manufacturing processes quality control. For a wide range of possible shifts and autocorrelation coefficients, performance comparisons between the neural-based algorithm, SCC chart, EWMAST chart, *X* chart and ARMAST are presented for ARMA(1,1) model. Guh (2008) presented a learning vector quantization (LVQ) based system that can effectively recognize CCPs in real time for various levels of autocorrelation for AR(1) model and compared its ARL performance with SCC chart, *X* chart and EWMA chart. Hwarng & Wang (2010) proposed a neural network based identifier (NNI) for multivariate autocorrelated processes. A rather extensive performance evaluation of the proposed scheme is carried out, benchmarking it against three statistical control charts, namely the Hotelling T^2 control chart, the MEWMA chart and the Z chart.

Over the last two decades, control charts for autocorrelated observations have been applied to an increasing number of real-world problems. In this section, control chart applications for the autocorrelated processes were reviewed, and the historical progression in this field was emphasized in order to help the interested researchers and practitioners get informed about the references on the relevant research in this field, regarding the design, performance and applications of control charts for autocorrelated processes. Recent research studies for autocorrelated data are summarized in Table 3.1 in a chronological order, in order to see the gradual development in these works.

Table 3.1 Evolution of control charts for autocorrelated data

Year	Author(s)	Control Charts	Autocorrelation Structure
1974	Johnson & Bagshaw	J&B	AR(1)
1988	Alwan & Roberts	Shewhart $\bar{x}$, CCC, SCC	IMA(1,1), ARMA(1,1)
1989	Yourstone & Mongomery	GMA, GMR	ARMA(2,1), AR(2)
1991	Harris & Ross	EWMA, CUSUM	AR(1)

1991	Montgomery & Mastrangelo	MCEWMA	AR(1)
1991	Yourstone & Mongomery	SACC, GACC	AR(4), ARMA(2,4)
1992	Wardell et al.	EWMA	ARMA(1,1)
1994	Wardell et al.	Shewhart $\bar{x}$, EWMA	AR(1)
1995	Mastrangelo & Montgomery	MCEWMA	IMA(1,1), ARIMA(1,1,1), AR(1), AR(2), ARMA(1,1)
1995	Runger & Willemain	R&W	AR(1)
1996	Runger & Willemain	UBM	AR(1)
1997	Kramer & Schmid	Shewhart $\bar{x}$	AR(1)
1997	Reynolds & Lu	EWMA	AR(1)
1997	Yang & Makis	Shewhart $\bar{x}$, CUSUM, EWMA	AR(1)
1997	Zhang	Shewhart $\bar{x}$	AR(2)
1997	Atienza et al.	SACC, SCC, CUSUM	AR(1), MA(1)
1998	Willemain & Runger	Run sum chart	AR(1), ARMA(1,1)
1998	Zhang	EWMAST	AR(1), AR(2), ARMA(1,1)
1999	Apley & Shi	Cuscore charts	ARIMA(4,0,3)
1999	Lu & Reynolds	EWMA	AR(1)
1999	West et al.	Multivariate Shewhart, MEWMA, BPN	VAR(1)
2000	Jiang et al.	ARMA, ARMAST, EWMAST, EWMA, CUSUM, Shewhart $\bar{x}$	AR(1), ARMA(1,1)
2000	Luceno & Box	One-sided CUSUM	AR(1)
2001	Jiang	ARMA	ARMA(1,1)
2001	Rao et al.	CUSUM	AR(1)
2001	Chiu et al.	BP Neural Network	AR(1)
2002	Jiang et al.	PID	ARMA(1,1)
2002	Kacker & Zhang	Shewhart $\bar{x}$	IMA(λ , σ)
2002	Shu et al.	CUSUM-triggered Cuscore	ARMA(1,1)
2003	Ben-Gal et al.	CSPC	AR(1), AR(2), MA(1)
2004	Winkel & Zhang	EWMA, EWMAST	AR(1)
2005	Snoussi et al.	Shewhart $\bar{x}$, CUSUM, EWMA, EWMA Q, CUSUM Q	AR(1)
2005	Winkel & Zhang	EWMAST, EWMA	AR(1)
2005	Kim et al.	MFC	AR(1)
2006	Yang & Yang	CSC, Shewhart- $\bar{x}$, Hottelling T^2	AR(1)
2006	Brence & Mastrangelo	MCEWMA	AR(1), ARMA(1,1)
2006	Noorossana & Vaghefi	MCUSUM	AR(1)
2006	Triantafyllopoulos	A new Multivariate Control Chart	AR(1)
2007	Kim et al.	DFTC	AR(1), AR(2)
2007	Ghourabi & Limam	Pattern Chart, SCC	AR(1)
2007	Pacella & Semeraro	SCC, *X* chart, EWMAST, ARMAST Elman NN	ARMA(1,1)
2008	Costa & Claro	DS $\bar{x}$	ARMA(1,1)
2008	Zou et al.	VSIFT $\bar{x}$, VSRFT $\bar{x}$	AR(1)
2008	Cheng & Chou	ARMA	ARMA(1,1)
2008	Issam & Mohamed	MCUSUM	VAR(1)
2008	Koksal et al.	Residual chart, modified Shewhart, EWMAST, ARMA	AR(1)
2008	Guh	SCC, *X* chart, EWMA, LVQ NN	AR(1)
2009	Weiss & Testik	CUSUM	Poisson INAR(1)
2009	Sheu & Lu	GWMA, EWMA	AR(1)
2009	Knoth et al.	Shewhart, EWMA	AR(1)
2010	Hwarng & Wang	Hotelling T^2, MEWMA, Z chart, NN Identifier	VAR(1)

We briefly summarize our conclusions from this detailed review in the following:

- Since the first control chart is proposed by Shewhart in 1931, lots of charts have been developed and then improved to be used for different process data.

- Control charts for autocorrelated processes attracted scientists' attention in 1970s. Scientists studied the effect of autocorrelation on the existing charts, initially. Later, they proposed charts for autocorrelated data.

- Many scientists have studied the residual control charts more than modified charts due to their simplicity. Scientists proposed original and innovative control charts in earlier years. But in recent years most of the proposed control charts are enhanced versions of existing charts.

- According to the Table 3.1 AR(1) and ARMA(1,1) processes are the most commonly used models in the literature.

2.4 Regression Control Chart

In this subsection the basic concepts of linear regression are explained before discussing conventional regression control chart and a brief review on regression control chart is given.

2.4.1 Linear Regression

In many problems two or more variables are inherently related, and it is necessary to explore the nature of this relationship. Regression analysis is a statistical technique for modeling and investigating the relationship between two or more variables (Montgomery & Runger, 1999). Regression chart is designed to control a varying (rather than a constant) average, and assumes that the values of the dependent variable are linearly (causally) related with the values of the independent variable. Note that control limits of conventional regression control chart are

regression lines. In statistics, linear regression is a regression method that models the relationship between a dependent variable (*y*), independent variable (*x*) and a random term ε :

$$y_t = \beta_0 + \beta_1 x_{t1} + \beta_2 x_{t2} + ... + \beta_m x_{tm} + \varepsilon_t \qquad t = 1, 2, ..., N \tag{2.26}$$

where the error ε_t is assumed to be an independently and identically distributed normal variable with a mean of zero and constant variance σ^2. The first subscript (*t*) denotes the index of the observation and the second subscript (*m*) denotes the index of the input quality characteristic (Shu, Tsung, & Kapur, 2004). Simple linear regression considers a *single regressor* or *predictor x* and a dependent or *response* variable *y*. It is assumed that each observation, *y*, can be described by the model (Montgomery & Runger, 1999) given in Equation (2.27).

$$y = \beta_0 + \beta_1 x + \varepsilon \tag{2.27}$$

In simple linear regression it is aimed to find the straight line for which the differences (or residuals) between the actual values of y_t and the predicted values $\hat{y}_t$ from the fitted model are as small as possible. A mathematical technique which determines the values of β_0 and β_1 other than those determined by the least squares method would lead to a greater sum of squared differences between the actual and predicted values of *y* (Levine, Ramsey, & Berenson, 1995). The estimates of β_0 and β_1 should result in a line that is (in some sense) a "nest fit" to the data. The German scientist Karl Gauss (1977-1855) proposed estimating the parameters β_0 and β_1 in Equation (2.29) and (2.30) in order to minimize the sum of the squares of the vertical deviations in estimated regression model (Montgomery & Runger, 1999).

$$\hat{y}_t = \hat{\beta}_0 + \hat{\beta}_1 x_t + \varepsilon_t, \qquad t = 1, 2, ..., N \tag{2.28}$$

The *least square estimates* of the β_0(intercept) and β_1(slope) in the simple linear regression model are

$$\hat{\beta}_1 = \frac{\sum_{t=1}^{N}(y_t - \bar{y})(x_t - \bar{x})}{\sum_{t=1}^{N}(x_t - \bar{x})^2} \tag{2.29}$$

$$\hat{\beta}_0 = \bar{y} - \hat{\beta}_1 \bar{x} \tag{2.30}$$

where $\bar{y} = (1/N)\sum_{t=1}^{N} y_t$ and $\bar{x} = (1/N)\sum_{t=1}^{N} x_t$ (Montgomery & Runger, 1999).

The residual describes the error in the fit of the model to the *t*th observation y_t. Residuals are calculated by the formula $\varepsilon_t = y_t - \hat{y}_t$.

2.4.2 Conventional Regression Control Chart

If independent process data exhibit an underlying trend due to systemic causes, usually control charts based on ordinary least squares (OLS) regression are used for monitoring and control. The traditional control charts with horizontal control limits and a center line with a slope of zero have proven unreliable when systemic trend exists in process data. A device useful for monitoring and analyzing processes with trend is the regression control chart. A regression based control chart which is the combination of the conventional control chart and regression analysis was first proposed by Mandel in 1969. This chart is designed to control a varying (rather than a constant) average, and assumes that the values of the dependent variable are linearly (causally) related with the values of the independent variable. This chart assumes that the *y* values (the dependent variable) are linearly related (causally) to the *x* values (the independent variable). For each specific *x* value, it is assumed that the *y* values are normally and independently distributed with a mean value estimated from the regression line, and with a standard error which is independent of the value

of *x* and is estimated from the deviations of the actual observations from the *y* values estimated from the regression line. Mandel used simple linear regression for this chart. Rather than using standard control charts, practitioners typically implement regression based control charts to monitor a process with systemic trend (Utley & May, 2008). Quesenberry (1988) points out that these approaches essentially assume that resetting the process is expensive and that they attempt to minimize the number of adjustments made to keep the parts within specifications rather than reducing overall variability.

A regression control chart that integrates linear regression and control chart theory has proven useful and applicable in a wide variety of applications, as it requires only a least squares regression computer programme to process the data prior to constructing the control chart (Shu, Tsung, & Tsui, 2004). However, since the Mandel's regression control chart was developed for independent data, it is not an effective tool for monitoring process shift in autocorrelated process observations.

2.4.3 A Review on Regression Control Charts

A regression based control chart which is the combination of the conventional control chart and regression analysis was first proposed by Mandel in 1969. Mandel used regression control chart to monitor the variety of postal management problems. The modified regression control chart is also used when the process exhibits tool wear (Montgomery, 1997), (see also Duncan (1974) and Manuele (1945) for a detailed discussion on control charts for tool wear). Mandel also devised a simplification of the regression control chart. The simplification functioned as a residual chart because the values that were plotted on it were the residuals from the regression analysis (Utley & May, 2009). Zhang adopted Mandel's idea of a residual control chart for statistical process control data to the cause selecting chart (CSC) in 1984. The CSC, which is a type of a regression based control chart, is constructed for an outgoing quality characteristic only after it has been adjusted for the effect of incoming quality characteristic. Hawkins (1991) developed a procedure called regression adjustment. The scheme essentially consists of plotting univariate control

charts of the residuals from each variable obtained when that variable is regressed on all the others (Montgomery, 2009). A very important application of regression adjustment occurs when the process has a distinct hierarchy of variables, such as a set of input process variables and a set of output variables. Sometimes this situation is called a cascade process. If the proper set of variables is included in the regression model, the residuals from the model will typically be uncorrelated, even though the output variable exhibited correlation. The regression adjustment procedure has many possible applications in chemical and process plants where there are often cascade processes with several inputs but only a few outputs, and where many of the variables are highly autocorrelated at low lags (Montgomery, 2009). Two years later, Hawkins applied regression control chart to cascade processes and cited CSC as a particularly useful methodology for controlling quality in cascade processes. If linear regression is used to model a cascade process, then the values plotted on the cause selecting control chart are actually the standardized residuals from the regression relationship (Sulek, Marucheck & Lind, 2006). In the same year, Wade & Woodall (1993) reviewed the concepts of the CSC and examined the relationship between the CSC and multivariate Hotelling T^2 chart. In their opinion, the cause selecting approach is an improvement over the use of separate Shewhart control charts for each of two related quality characteristics. A review of the literature on control charts for multivariate quality control (MQC) is given by Lowry & Montgomery (1995), by discussing principal components and regression adjustment of variables in MQC. Haworth (1996) used a multiple regression control chart to manage software maintenance. A quality control tool was developed for managers of complex software maintenance processes that can be modeled with a multiple regression model. Kalagonda & Kulkarni (2003) proposed a diagnostic procedure called '*D*-technique' to detect the nature of shift. For this purpose, two sets of regression equations, each consisting of regression of a variable on the remaining variables, are used to characterize the 'structure' of the 'in-control' process and that of the 'current' process. To determine the sources responsible for an out-of-control state, it is shown that it is enough to compare these two structures using the dummy variable multiple regression equation. In the same year, Omura & Steffe (2003) constructed Mandel's regression control chart for apparent viscosity and average shear rate data. According

to the authors, no standardized test existed to objectively assess flow behavior of fluid foods with large particulates. Therefore, to monitor the process data using a regression control chart could be useful for quality control. In the following year; Shu, Tsung, & Tsui (2004) studied the run-length performance of EWMAREG (EWMA chart for regression residuals) and SheREG (Shewhart chart for regression residuals) with estimated parameters of regression equation, and used these charts for monitoring multistage processes where process data usually follow a multivariate normal distribution. The authors also studied the run length performance of regression control charts. However, Zhang (1984) and Wade & Woodal (1993) considered the CSC with sample size one, while the studies about construction of cause-selecting charts with sample size greater than one are discussed by Yang (2005) for joint $\bar{x}$ and $\bar{e}$ cause-selecting charts. Yang & Yang (2005) considered the problem of monitoring the mean of a quality characteristic x on the first process step, and the mean of a quality characteristic y on the second process, in which the observations x can be modeled as an ARMA model and observation y can be modeled as a transfer function of x since the state of the second process is dependent on the state of the first process. In the following year (in 2006) they addressed the $\bar{x}-s^2$ and $\bar{e}-s_e^2$ charts for two dependent process steps with over-adjusted means and variances. Sulek, Marucheck, & Lind (2006) examined the CSC as a methodology to monitor and identify potential problem areas in an actual cascade service process. The authors utilized the CSC as an appropriate methodology for analyzing the performance of a down stream stage in a multistage process by controlling the effect of performance in the upstream stage. Yang & Su (2007) constructed an adaptive sampling interval Z_x control chart to monitor the quality variable produced by the first process step, and used the adaptive sampling interval Z_e control chart to monitor the specific quality variable produced by the second process step. Asadzadeh, Aghaie, & Yang (2008) reviewed CSC for monitoring and diagnosing multistage processes. The following year (in 2009) they proposed a robust CSC to monitor multistage processes where outliers are presented in historical dataset. In the same year, Yang & Chen constructed the variable sampling interval (VSI) $Z_{\bar{x}}-Z_{s^2}$ and $Z_{\bar{e}}-Z_{s_{e^2}}$ control charts in order to effectively monitor the quality

variable produced by the first process step with incorrect adjustment and the quality variable produced by the second process step with incorrect adjustment, respectively. When the residual terms are not normally distributed, an alternative method for estimating the regression line is needed. One alternative method is the least absolute value (LAV) regression model. In contrast to the OLS approach, which minimizes the sum of the squared residuals, the LAV model minimizes the sum of the absolute values of the residuals. Utley & May (2009) proposed a control chart methodology for residual control charts that is based on least absolute value (LAV) regression.

In this section, control charts for autocorrelated processes and conventional regression control chart were reviewed, and the historical progression in this field was emphasized. Brief information about artificial neural networks is given in the following chapter. In this thesis, neural networks are used to recognize the autocorrelated and trended process observations before using proposed regression control chart.

CHAPTER THREE

PROPOSED REGRESSION CONTROL CHART FOR AUTOCORRELATED DATA (RCCA)

In this thesis, a new regression control chart for autocorrelated process observations (RCCA for short) which is able to detect the mean shift in a production process is presented. This chart is designed for autocorrelated process observations having a linearly increasing trend. Existing approaches may individually cope with autocorrelated and trending data. To the best of our knowledge there appears to be no chart that directly monitors the original data which exhibit both increasing linear trend and serial correlation. The proposed chart (RCCA) requires the identification of trend AR(1) model as a suitable time series model for process observations. For a wide range of possible shifts and autocorrelation coefficients, performance of the RCCA is evaluated by simulation experiments. Simulation results are given in chapter four. The average correct signal rate and the simulated average run length are used as performance criteria. Recognition of autocorrelated and trending process observations is performed by using neural networks. Next subsection describes the integrated neural based structure that we used to diagnose autocorrelation through the trending process observations. After presenting the neural based pattern recognizer, construction steps of the proposed chart will be given with an illustrative example.

3.1 Recognition of Autocorrelated and Trending Data Using Neural Networks

3.1.1 Background

In this subsection, before implementing RCCA, design and implementation of the combined neural network structure (CNN), that is composed of appropriate number of linear vector quantization (LVQ) and multi layer perceptron (MLP) (also known as the ‘feedforward backpropagation network’) neural networks that are used to recognize the trend in process data, is described. After recognizing the trending pattern, the Elman’s recurrent neural network (ENN) is used to diagnose the

autocorrelation through the trending data. When the literature is reviewed, it is observed that there is not any integrated neural network structure that combines LVQ, MLP and Elman networks together to recognize the autocorrelated and trending patterns. The proposed control chart can be employed to detect the shift in process data after recognition of autocorrelated and trending pattern as described in section 3.2 and section 3.3 with an illustrative example.

Researchers have investigated the use of artificial neural networks (NNs) in the application of control chart pattern recognition (CCPR) (Guh, 2008). Different statistical tools (such as least squares for trend analysis and time series analysis for calculating autocorrelation coefficients) can be easily implemented to process data to recognize the trend or autocorrelation in process data but when compared to other methodologies the neural network approach has certain advantages which are mentioned in section 2.3. The Appendix 1 describes in detail the process simulator for generating the CCP examples and etc. In recognition problems, NNs can recall patterns learned from noisy or incomplete representations, which makes them suitable for CCPR because CCPs are generally contaminated by common cause variations (Guh, 2008). Pattern recognition provides a mechanism for identifying different types of predefined patterns in real time on the series of process quality measurements. The recognized patterns then serve as the primary information for identifying the causes of unnatural process behavior (Pacella & Semeraro, 2007).

Various studies have demonstrated the utility of NNs in identifying CCPs. Pham & Oztemel (1992a, 1994) used a backpropagation network (BPN) and learning vector quantization (LVQ) network to recognize shift, trend and cycle patterns on control charts. Their Back Propagation (BP) and LVQ networks achieved 95% and 97.7% accuracy, respectively. Hwarng & Hubele (1993) extensively investigated CCPR by training back propagation networks (BPNs) to detect six unnatural CCPs suddenshift, trend, cycle, stratification, systematic, and mixture. Cheng (1997) developed a NN approach for the analysis of control chart patterns. Anagun (1998) organized the training data in two different ways (direct representaion and histogram representation) before introducing them to the designed NN applied to pattern

recognition in statistical process control. Guh & Tannock (1999) tried to investigate the feasibility of an NN to recognize concurrent control chart patterns (where more than one pattern exists together, which may be associated with different causes). Pham & Chan (2001) described in their paper, the use of unsupervised adaptive resonance theory ART2 neural networks for recognizing patterns in statistical process control charts. Pham & Sagiroglu (2001) presented an overview of four algorithms used for training MLP networks and the results of applying those algorithms to teach different MLPs to recognise control chart patterns and classify wood veneer defects. The algorithms studied are BP, Quickprop (QP), Delta-Bar-Delta (DBD) and Extended-Delta-Bar-Delta (EDBD). The results have shown that, overall, BP was the best algorithm for the two applications tested. Al-Assaf (2004) used multi-resolution wavelets analysis (MRWA) to extract distinct features for unnatural patterns by providing distinct time-frequency coefficients. Gauri & Chakraborty (2006) developed two feature-based approaches using heuristics and articial neural network, which are capable of recognizing eight most commonly observed CCPs including stratication and systematic patterns. In the following year (2007), they presented potentially useful 32 features which provide an opportunity for understanding the behaviours of the CCPs in detail. They demonstrated a simple approach for designing the optimal feature-based heuristic using the classification and regression trees (CART) algorithm, which is capable of detecting all of the eight basic CCPs using a considerable smaller number of observations. Gauri & Chakraborty (2008) selected a set of seven shape features so that their magnitudes will be independent of the process mean and standard deviation. Based on these features, all the eight commonly observed CCPs are recognized by using a MLP. Jiang, Liu, & Zeng (2009) used a BPN to recognize control chart patterns preliminarily and then they adopted numerical fitting method to estimate the parameters and specific types of the patterns, which is different from the traditional neural network-based control chart pattern recognition methods. Recently, pattern recognition techniques based on artificial neural network (ANN) are limited to recognize simple CCPs arising from single type of unnatural variation. In other words, they are incapable to handle the problem of concurrent CCPs where two types of unnatural variation exist together within the manufacturing process. Wang, Dong,

& Kuo (2009) presented a hybrid approach based on independent component analysis (ICA) and decision tree (DT) to identify concurrent CCPs. Without loss of generality, six types of concurrent CCPs are used to validate the proposed method. Recognition of various control chart patterns (CCPs) can significantly reduce the diagnostic search process. Feature-based approaches can facilitate efficient pattern recognition. In the same year, a set of seven most useful features is selected by Gauri & Chakraborty (2009), using a classification and regression tree (CART)-based systematic approach for feature selection. Based on these features, eight most commonly observed CCPs are recognized using heuristic and MLP network.

Figure 3.1 displays the NN aided pattern recognition and process monitoring procedure of the RCCA. As can be seen, for recognizing the trend and autocorrelated patterns, a combined NN architecture is used to provide a collective authority in decision for trended data, and call it combined neural network recognizer (CNNR), then employ ENN to recognize the autocorrelation that is filtered by CNNR.

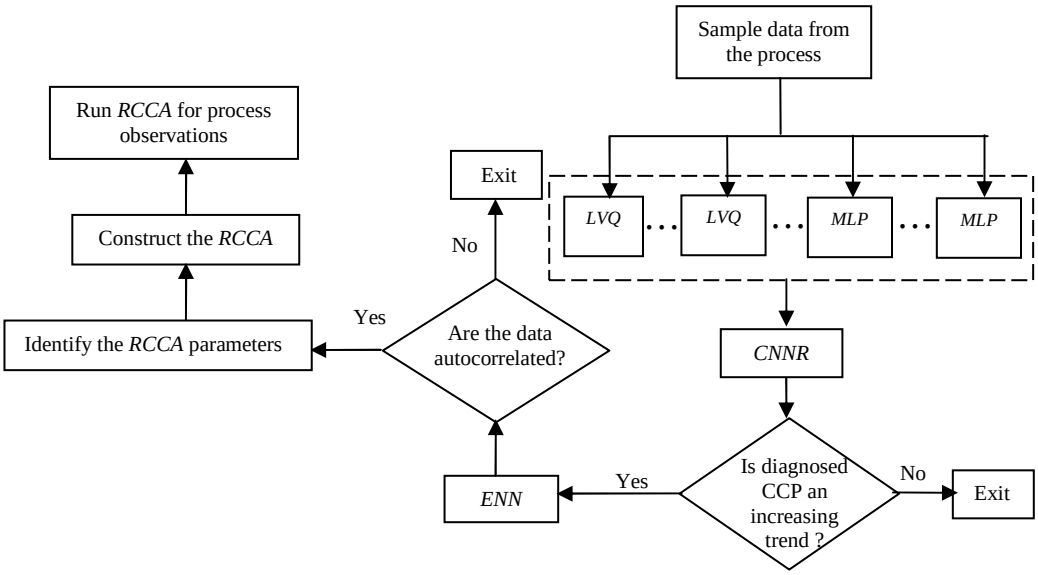

Figure 3.1 NN aided pattern recognition and process monitoring procedure of the RCCA.

Topologies of MLP and LVQ are given in Figure 3.2 and Figure 3.3, respectively. Each neuron, represented by truncated cylinders in a layer, is connected with all neurons of the next layer by arcs. Each arc has a weight. Threshold value prevents the neurons to produce zero value. In Figure 3.3, the weights of arcs

between Kohonen and output layers are equal to one (see Oztemel (2003) and Gauri & Chakraborty (2008) for details). The output of MLP and LVQ is one of the control chart patterns (CCP). The desired CCP for LVQ and MLP for the input data under consideration is increasing linear trend that is one of the six CCP types (naturel pattern: NP; upward shift: US; downward shift: DS; increasing trend: IT; decreasing trend: DT; periodic shift: PS).

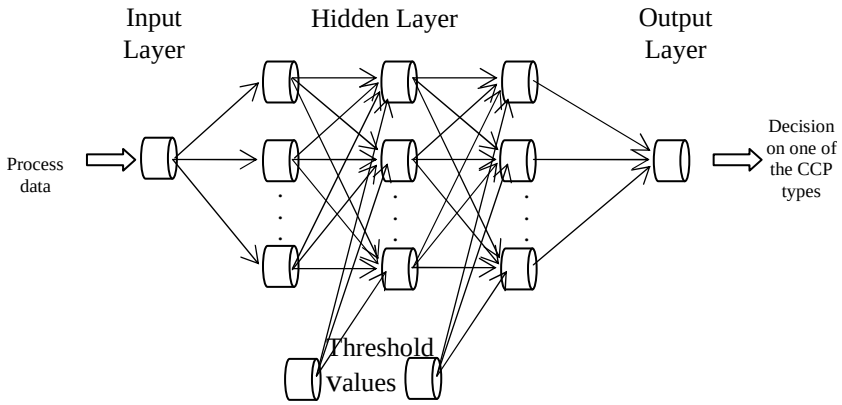

Figure 3.2 Feedforward MLP NN architecture (Oztemel, 2003; Gauri & Chakraborty, 2008).

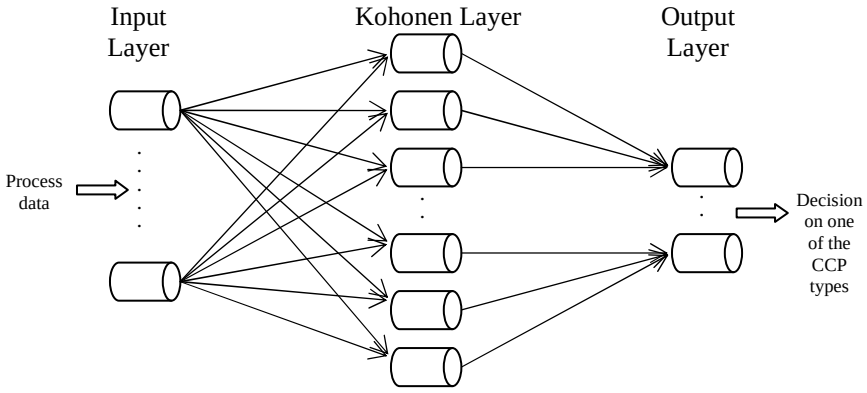

Figure 3.3 LVQ NN architecture (Oztemel, 2003; Ham & Costanic, 2001).

Learning rules of MLP and LVQ networks are given in Appendix 2 and Appendix 3, respectively. The combined NNs that consist of three or more NNs give more successful solutions when compared with single NN structure (Oztemel, 2003). The inputs are presented to each NN independently and also each NN are trained independently, and the outputs of them are obtained. In this thesis appropriate

numbers of LVQ and MLP networks are combined to obtain more successful solutions. Components of CNNR are displayed in Figure 3.4. Each of the NN was trained independently from others. The outputs of these NNs were combined and by the help of a collective decision making module (CDMM) a collective decision was performed. A CDMM depends on unanimity.

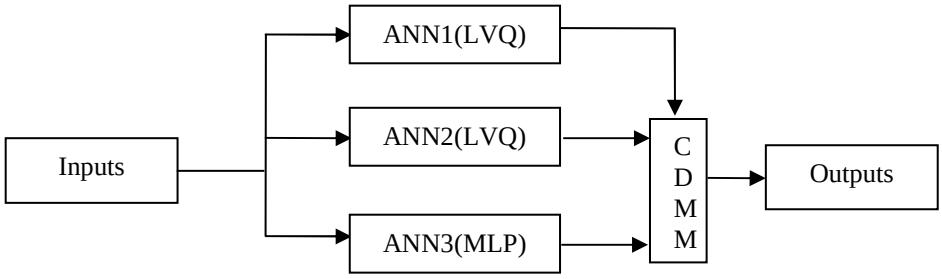

Figure 3.4 Components of the CNNR.

Operation of CDMM is given in Appendix 4. After recognizing the trended pattern, the Elman's recurrent neural network (ENN) was used to diagnose the autocorrelation through the trending data. A recurrent ENN where the recurrency allows the network to remember cues from the recent past is suitable for recognizing time series data and monitoring process shifts in the presence of autocorrelation (Pacella & Semeraro, 2007). ENN is especially used for modeling first ordered linear systems. ENN has the ability of processing the data that are time dependent and also can transform the results that are obtained at previous time to a one step ahead. ENN considers relations that are time dependent. So this network is used to estimate the future by considering its behaviours today (Oztemel, 2003). ENN is similar to MLP when its construction is considered but differs from MLP at having the dynamic memory property which brings this algorithm a special importance to recognize time series data. The ENN employs feedback connections and addresses the temporal relationship of its inputs by maintaining an internal state. In ENNs input layer does not include transfer function like MLP. Topology of ENN is given in Figure 3.5. Learning rules of ENN are given in Appendix 5. The output of ENN is that if the trended process data filtered by CNNR is autocorrelated or not.

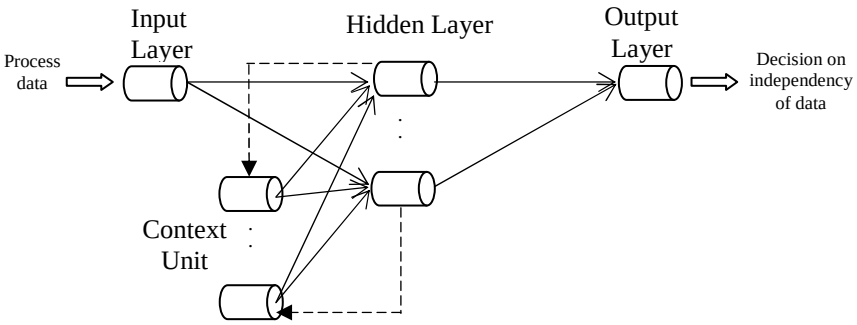

Figure 3.5 ENN architecture (Ham & Kostanic, 2001; Oztemel, 2003).

In the relevant literature, for the autocorrelated processes, NNs are used to recognize if the input pattern is one of the CCP types (first task) and is it autocorrelated (second task), simultaneously. Because of the complexity of autocorrelated processes with one of CCP types, the training process of networks can be hard, while the correct classification rate decreases. By the proposed integrated structure, the mentioned two tasks are distributed to different networks. The first task is performed by CNNR that is composed of appropriate number of LVQ and MLP networks, while the second task is performed by the ENN that is advisable to recognize autocorrelation. Executing only one of the given tasks, correct classification rate of each network increases and training these networks are simplified; and then by combining the results of each network, the performance of proposed network structure is increased when it is compared with the results represented in the literature.

3.1.2 Generating Sample Data

In this section how training and testing data sets are generated is explained. Generated data sets are used in training and testing the networks and also calculating the performance of RCCA. The process simulator coded in MATLAB 7.4.0 was used for generating the training data sets. The details of process simulator are given in Appendix 1.

3.1.2.1 Training Data Set for CNNR

For each type of the six CCPs 400 sample data sets were generated. Each data set is composed of 500 observations. While one half of the sets are uncorrelated, the other half contains both correlated and uncorrelated data sets. The former sets are collected in set1, and the latter in set2. For each CCP type in set2, 40 data sets were generated using each of five ϕ values such as 0.95, 0.475, 0.0, -0.475, and -0.95. That is, the first 40 sets were simulated using ϕ=0.95, the second 40 sets for ϕ=0.475, and so on. Set1 and set2 were generated by different process simulators that are given in Appendix 1. Set1 and set2 were used together for training of MLP and LVQ. Parameter values used for process simulator are displayed in Table 3.1.

Table 3.1 Details of the CCP training example sets for the LVQ and MLP networks

Pattern type	Parameter range for *set1*	Parameter range for *set2*	Set name and number of observations
Normal distribution	$t=[1,500]$, $\mu=10$, $\sigma=2$, $u=Uniform[0,1]$	$t=[1,500]$, $\xi=0$, $x_1=10$, $\varepsilon \sim N(0,4)$, $\phi: 0.95, 0.475, 0.0, -0.475, -0.95$	Set1:200 Set2:200
Increasing trend	$g=uniform[0.1,0.125]$ (for the first 100 data set) $g=0.2$ (otherwise)	$d=0.2$	Set1:200 Set2:200
Decreasing trend	$(-g)$	$(-d)$	Set1:200 Set2:200
Sliding up	$k_{sliding}=0$ (if $t<50$) $k_{sliding}=1$ (if $t\geq 50$) $s_{displacement}=Uniform[2,4]$	$k_{sliding}=0$ (if $t<150$) $k_{sliding}=1$ (if $t\geq 150$) $s_{displacement}=(4.5)$	Set1:200 Set2:200
Sliding down	$(-k_{sliding})$	$(-k_{sliding})$	Set1:200 Set2:200
Periodical shifting	$N=500$ $\pi=500$ $\alpha_{periodic}$ = randint [0,30]	$N=500$ $\pi=500$ $\alpha_{periodic}$ =(0.25,1.0,3.0)	Set1:200 Set2:200

3.1.2.2 Training Data Set for ENN

To train ENN, both autocorrelated and uncorrelated data sets, with increasing and decreasing linear trend, were generated. Each set is composed of 500 data points. Underlying model for autocorrelated process is given in Appendix 1. Totally 800 sets were generated for autocorrelated process; one half for increasing trend and other

half for decreasing trend. On the other hand, each 100 of autocorrelated sets have a specific ϕ value ($\phi: 0.95, 0.475, -0.475, -0.95$) listed in Table 3.2. Underlying model for uncorrelated process with increasing trend is given below.

$$X_t = \mu_t + \varepsilon_t + dt \tag{3.1}$$

For the process with decreasing trend sign of the dt in Equation (3.1) will be negative. 400 sets were generated for each of uncorrelated process with increasing trend and decreasing trend, respectively. Parameter values used for CCP training data sets are depicted in Table 3.2.

Table 3.2 Details of the CCP training example set for the ENN

Parameter range for AR(1) process data	Parameter range for uncorrelated process data
$\xi = 0,\ x_1 = 10,\ \varepsilon \sim N(0,4),\ t = [1,500]$	$\varepsilon \sim N(0,4),\ t = [1,500]$
$\phi: 0.95, 0.475, -0.475, -0.95$	
$d = 0.2$ (for increasing trend)	$g = 0.2$ (for increasing trend)
$(-d)$ (for decreasing trend)	$(-g)$ (for decreasing trend)

3.1.3 Recognition of Trend and Autocorrelation in Data

3.1.3.1 CNNR to Detect Six Unnatural CCPs

Three different ANN based recognizers were developed. First two of these recognizers (ANN1 and ANN2) use LVQ algorithm. Architectures of ANN1 and ANN2 differ in number of neurons at Kohonen layer. The third member of CNNR uses MLP structure. Configurations of the LVQ and the MLP networks which are the members of the CNNR are depicted in Table 3.3 and Table 3.4, respectively. Preliminary investigations are conducted to choose a suitable network topology and training algorithm for each member of CNNR. According to the experimental design performed for investigating the appropriate network topologies of LVQ networks, the design parameters for learning rate (0.01, 0.03, 0.06, 0.09) respect to number of neurons at Kohonen layer (from 4 to 40 neurons increasing four by four) are used and minimum mse (mean square error) is reached with the design parameters that are given in Table 3.3. Similarly, for MLP network, the design parameters for number of

hidden layers (from 1 to 4 increasing one by one), number of neurons at each layer (from 8 to 72 increasing eight by eight), learning rates (0.01, 0.02) and momentum constants (from 0.02 to 0.05 increasing with step size 0.01) are used and minimum mse is reached for the design parameters that are given in Table 3.4.

Table 3.3 Network configurations for LVQ NNs

Members of CNNR :	ANN1	ANN2
Type of ANN	LVQ	LVQ
Number of neurons at Kohonen layer	24	36
Learning rate	0.01	0.01
Training example set	Set1+ Set2	Set1+ Set2
Training example set class percentages	are same and equal to (1/6) for each of six CCP type	
Network training parameters		
Error goal :	$1x10^{-17}$ (1e-17)	$1x10^{-17}$ (1e-17)
Maximum number of epochs :	200	200

Table 3.4 Network configuration for MLP NN

Members of CNNR :	ANN3
Type of ANN	MLP
Number of hidden layers	3
Number of neurons at each hidden layer respectively	12, 64, 64
Number of neurons at output layer	1
Functions	
Transfer (activation) functions of hidden layers respectively:	Purelin, Tangent sigmoid, Tangent sigmoid
Transfer (activation) function of output layer :	Purelin
Backpropagation network training function :	TRAINGD Gradient descent back propagation
Backpropagation weight/bias learning function :	LEARNGD Gradient descent weight/bias learning function
Performance function :	mse (mean square error)
Training set	Set1+ Set2
Network training parameters	
Error goal :	$1x10^{-2}$
Maximum number of epochs :	30000
Momentum constant :	0.4
Learning rate :	0.01

The generated data were presented to each NN independently and also each NN was trained independently. The coding is performed in MATLAB 7.4.0. Then outputs of these NNs were combined and by the help of a collective decision making module (CDMM) a collective decision is performed (see Oztemel (2003) and Gauri & Chakraborty (2008) for detailed information). The training was stopped whenever either the error goal is achieved or the maximum allowable number of training epochs is met. Now verification sets are needed for testing the performance of NNs

which are the members of CNNR. New sets of verification samples of size 2400 each were generated by using the parameters given in Table 3.1 again. The generated samples for verification were used to test the performance of CNNR members. The recognition performance of all these ANN-based recognizers was tested using different sets of test samples. The verification results of the ANN-based recognizers are displayed through Table 3.5 - Table 3.7, and the performance of CNNR is given in Table 3.8. The elements in these tables are the classification rates (CR) of networks by percentages. The columns represent the expected classification for the input pattern, while rows represent the actual classification rate of network for the given test set. For example in Table 3.5, for the first column the expected classification is NP, but as it can be seen from the last row of Table 3.5, the correct classification rate of ANN1 is 92.5%.

Table 3.5 Testing results of the ANN1 for autocorrelated data

CR (%)		Required classification					
		NP	US	DS	IT	DT	PS
Network classification	PS	0.0000	0.0000	0.0000	0.0000	0.0000	0.7565
	DT	0.0000	0.0000	0.0052	0.0000	0.9982	0.0000
	IT	0.0000	0.0105	0.0000	0.9884	0.0000	0.0000
	DS	0.0750	0.0020	0.9848	0.0000	0.0018	0.0000
	US	0.0000	0.9875	0.0000	0.0116	0.0000	0.0000
	NP	0.9250	0.0000	0.0100	0.0000	0.0000	0.2435

NP: natural pattern; US: upward shift; DS: downward shift; IT: increasing trend; DT: decreasing trend; PS: periodic shift

Table 3.6 Testing results of the ANN2 for autocorrelated data

CR (%)		Required classification					
		NP	US	DS	IT	DT	PS
Network classification	PS	0.0000	0.0000	0.0000	0.0000	0.0000	0.7550
	DT	0.0000	0.0000	0.0010	0.0000	0.9975	0.0000
	IT	0.0000	0.0000	0.0000	0.9876	0.0000	0.0000
	DS	0.0600	0.0150	0.9990	0.0000	0.0025	0.0000
	US	0.0000	0.9850	0.0000	0.0124	0.0000	0.0000
	NP	0.9400	0.0000	0.0000	0.0000	0.0000	0.2450

NP: natural pattern; US: upward shift; DS: downward shift; IT: increasing trend; DT: decreasing trend; PS: periodic shift

Table 3.7 Testing results of the ANN3 for autocorrelated data

CR (%)		Required classification					
		NP	US	DS	IT	DT	PS
Network classification	PS	0.0000	0.0100	0.0000	0.0000	0.0000	0.9990
	DT	0.0000	0.0050	0.0100	0.0350	0.9950	0.0000
	IT	0.0050	0.0000	0.0000	0.9500	0.0000	0.0000
	DS	0.0000	0.0350	0.9900	0.0150	0.0050	0.0000
	US	0.0000	0.9500	0.0000	0.0000	0.0000	0.0000
	NP	0.9950	0.0000	0.0000	0.0000	0.0000	0.0010

NP: natural pattern; US: upward shift; DS: downward shift; IT: increasing trend; DT: decreasing trend; PS: periodic shift

Table 3.8 Testing results of the CNNR for autocorrelated data

CR (%)		Required classification					
		NP	US	DS	IT	DT	PS
Network classification	PS	0.0000	0.0000	0.0000	0.0000	0.0000	0.7650
	DT	0.0000	0.0000	0.0024	0.0000	0.9968	0.0000
	IT	0.0000	0.0090	0.0000	0.9947	0.0000	0.0000
	DS	0.0600	0.0000	0.9976	0.0000	0.0032	0.0000
	US	0.0000	0.9910	0.0000	0.0053	0.0000	0.0000
	NP	0.9400	0.0000	0.0000	0.0000	0.0000	0.2350

NP: natural pattern; US: upward shift; DS: downward shift; IT: increasing trend; DT: decreasing trend; PS: periodic shift

As can be seen from these tables, at the training and verification phases, recognition performances of three members of CNNR are good for trended patterns. The overall mean percentage values of correct recognition at the training and verification phases for trended patterns are highly correct for all NN based recognizers. As can be seen from Table 3.8, the correct classification rate of CNNR is higher then its members and 99.47% for increasing trend. These correctly recognized trended patterns are used as input for ENN.

3.1.3.2 Network Configuration of ENN

Configuration for ENN is given in Table 3.9. Initially, all weight values were chosen randomly and then they were optimized during the training stage.

Table 3.9 Network configuration for ENN

Number of neurons at each layer respectively	6 (for hidden layer), 1 (for output layer)
Functions	
Transfer (activation) function of hidden layer :	Tangent Sigmoid
Transfer (activation) function of output layer :	Purelin
Backpropagation network training function :	TRAINGDX Gradient descent w/momentum & adaptive lr backpropagation
Backpropagation weight/bias learning function :	LEARNGDM Gradient descent w/momentum weight/bias learning function
Performance function :	mse (mean square error)
Training example set :	Presented in Table 3.2
Network training parameters	
Error goal :	$1x10^{-2}$
Maximum number of epochs :	500

Desired output of ENN is either 1 if the autocorrelation has been detected or 0 otherwise. Due to the random noise and to different values of actual inputs, the output of ENN is a number ranging approximately between 0 and 1. Therefore, an

activation cut off value must be defined to release an alarm if the network output is greater than the cutoff. Similar to the approach used by Pacella & Semeraro (2007), we defined a cut off value (C) 0.60 for increasing trend and 0.5290 for decreasing trend. If the trained NN signals greater than or equal to cutoff value, point out that the tested data set has serial correlation, otherwise has no serial correlation.

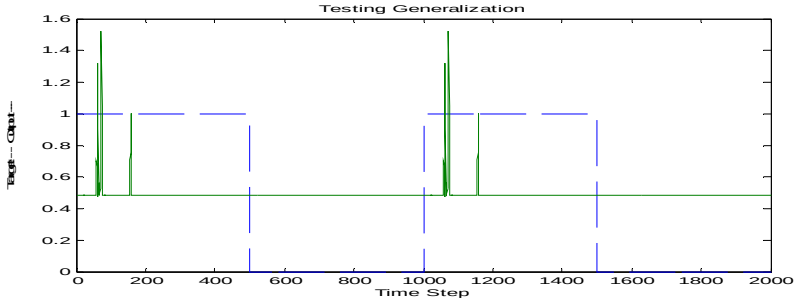

Figure 3.6 A test solution for an example test set of autocorrelated and uncorrelated trended data that have been shown to Elman NN twise.

Table 3.10 summarizes the performance of ENN for autocorrelated data with increasing linear trend that is filtered by CNNR.

Table 3.10 Testing results of the ENN

		Required classification	
		Autocorrelated	Uncorrelated
Network Classification	Autocorrelated	0.9846	0.0003
	Uncorrelated	0.0154	0.9997

The results displayed in Table 3.10 indicate that autocorrelated increasing trend is recognized with 98.46% accuracy rate for the cutoff value 0.60. This means that autocorrelation has been detected by ENN with 98.46% accuracy through the set that is correctly recognized by CNNR (see Table 3.10) with 99.47% accuracy from trend AR(1) test set. In this case the network did a fairly good job with only 6 neurons in the recurrent layer, and 500 training epochs. More recurrent neurons and longer training times could be used to increase the network's accuracy on the training data. Training the network on more amplitude will result in a network that generalizes better. Based on preliminary investigation, no evident improvement in performance was attained by extending the training set beyond 400 examples for each type.

3.2 Construction of the Proposed Chart

After the linear trend and serial correlation were diagnosed by means of NNs, the RCCA was used for different magnitudes of the mean shift, under the presence of various levels of autocorrelation. Performance of the RCCA was evaluated in terms of the average correct signal rate and the simulated average run length (ARL). An autoregressive process of lag 1, AR(1), is the representative model for autocorrelated processes. In an AR(1) process, the current observation is correlated with its previous observation. Past studies emphasize the role of AR(1) processes in process control (Guh, 2008). An AR(1) model can be expressed as follows:

$$x_t = \xi + \phi x_{t-1} + \varepsilon_t \tag{3.2}$$

where t is the time of sampling, x_t is the sample value at time t, ξ is the constant, ϕ is the autoregressive coefficient ($-1<\phi<1$), and ε_t is the independent random error term (common cause variation) at time t following $N=(0,\sigma_\varepsilon^2)$. Let autocorrelated process observations (x_t) with an increasing linear trend (trend AR(1) process) be represented by:

$$X_t = x_t + dt \tag{3.3}$$

where d is the trend slope and t is the time step (or observation number), and autocorrelated and trending process observations (X_t) with a mean shift be depicted by:

$$Z_t = X_t + \delta_\mu \tag{3.4}$$

where δ_μ is the magnitude of upward mean shift. In this thesis, our aim is to test for an upward shift in the mean of $\{Z_t\}$ by using the RCCA. Notations are listed in Appendix 6. The RCCA is constructed in the following five steps;

Step 1 Fit a simple linear regression model to the data.

The center line of the RCCA is a regression line as is in a conventional regression chart. So the parameters β_1 (slope) and β_0 (intercept) need to be estimated by

$$\hat{\beta}_1 = \frac{\sum_{t=1}^{N}(Z_t - \bar{Z})(t - \bar{T})}{\sum_{t=1}^{N}(t - \bar{T})^2} \tag{3.5}$$

$$\hat{\beta}_0 = \bar{Z} - \hat{\beta}_1 \bar{T} \tag{3.6}$$

where N represents the sample size, Z_t is the tth observation, $\bar{Z}$ the mean value of Z_t, $t=1,2,\ldots,N$ and $\bar{T}$ the mean value of t

$$\bar{Z} = \frac{\sum_{t=1}^{N} Z_t}{N} \quad \text{and} \quad \hat{\sigma} = \sqrt{\frac{\sum_{t=1}^{N}(Z_t - \bar{Z})^2}{N-1}} \tag{3.7}$$

$$\bar{T} = \frac{\sum_{t=1}^{N} t}{N} \tag{3.8}$$

Step 2 Calculate the RCCA variation parameter (RCCAVP for short).

$$RCCAVP = \sqrt{\hat{\sigma}_e \left(\frac{1}{1-\phi^2} \right)} \tag{3.9}$$

where

$$\hat{\sigma}_e = \sqrt{\frac{\sum_{t=1}^{N}(e_t - \bar{e})^2}{N-1}} \tag{3.10}$$

is the standard deviation of $\{e_t\}$ which is the difference between expected and observed values of Z_t,

$$e_t = Z_t - \phi Z_{t-1}, \tag{3.11}$$

and $\bar{e}$ is the sample mean of $\{e_t\}$

$$\bar{e} = \frac{\sum_{t=1}^{N} e_t}{N} \tag{3.12}$$

Step 3 Calculate the time dependent EWMAARZ parameter to widen the control limits up. The aim is to obtain an acceptable false alarm rate.

$$\text{EWMAARZ} = \sqrt{\frac{\sum_{t=1}^{N} \hat{\sigma}_{EWMA(t)}}{N}} \tag{3.13}$$

where

$$\hat{\sigma}_{EWMA(t)} = \alpha e_t^2 + (1-\alpha)\hat{\sigma}_{EWMA(t-1)} \tag{3.14}$$

and $\hat{\sigma}_{EWMA(1)} = \hat{\sigma}_e$. During the comprehensive experiments we conducted, it is observed that the RCCA gives better performance for α=0.80. $\hat{\sigma}_{EWMA}$ is the estimated smoothed standard deviation of Z_t and shows similar characteristics with the smoothed variance in moving centerline EWMA (MCEWMA) chart. As can be seen in (3.13), EWMAARZ is affected by the process residuals, and implicitly by the autoregressive parameter ϕ. As depicted in Equation (3.11), residuals get larger for ϕ < 0 and vice versa.

Step 4 Calculate $\overline{C}^{+}$ ($\overline{C}^{-}$) to widen (narrow) the upper control limit if there is an upward (downward) shift in the mean of the process.

There is an upward (downward) shift in the process mean if $\overline{C}^{+}$ ($\overline{C}^{-}$) continues to get larger (smaller).

$$\overline{C}^{+} = \frac{\sum_{t=1}^{N} C^{+}_{RCCA(t)}}{N} \tag{3.15}$$

$$\overline{C}^{-} = \left| \frac{\sum_{t=1}^{N} C^{-}_{RCCA(t)}}{N} \right| \tag{3.16}$$

where $C^{+}_{RCCA(1)} = 0$, $C^{-}_{RCCA(1)} = 0$, $C^{+}_{RCCA(t)} = \left\{ \max[0, Z_t - (\hat{M}^{t}_{o} + k)] \right\}$,

$$C^{-}_{RCCA(t)} = \left\{ \min[0, Z_t - (\hat{M}^{t}_{o} - k)] \right\} \tag{3.17}$$

and

$$\hat{M}^{t}_{o} = \phi^2 \frac{D_o}{2} + \hat{\beta}_1 t \qquad t = 1, 2, ..., N \tag{3.18}$$

denotes the target varying mean for process observations at each time step *t.* In the CUSUM control chart, deviations from the constant target mean (μ_0) are used to calculate accumulating deviations. In the present dissertation, with a similar purpose, $\hat{M}^{t}_{o}$ is used as a reference value for the process observations. The distance between each process observation and $\hat{M}^{t}_{o}$ is calculated in each time step *t*. On the other hand, if the conventional regression control chart that is proposed by Mandel is considered,

the center line formulated by $y = \hat{\beta}_0 + \hat{\beta}_1 t$ also represents the target varying mean. Intercepts show difference between $\hat{M}_o^t$ and the target varying mean in the Mandel's regression control chart.

The intercept in $\hat{M}_o^t$ is formulated as $\phi^2 \frac{D_o}{2}$. Calculations for D_o are given in Table 3.11. For positive autocorrelation, because of the nature of the process, a relatively large observation at the previous time step tends to be followed by another large value at the current time step. RCCA adjusts its control limits' width with respect to the autocorrelated process observations by using $\overline{C}^+$ and $\overline{C}^-$. For this purpose, RCCA takes into consideration the sign of autocorrelation and the magnitude of autocorrelation coefficient. The functional role of $\overline{C}^+$ and $\overline{C}^-$, that are the means of calculated $C^+_{RCCA(t)}$ and $C^-_{RCCA(t)}$ values, will be given in detail at the following pages. As mentioned before $C^+_{RCCA(t)}$ and $C^-_{RCCA(t)}$ represent derivations from the target varying mean at each time step *t*. By using $\overline{C}^+$ and $\overline{C}^-$ the width of the control limits are decreased. In other words, $\overline{C}^+$ and $\overline{C}^-$ have decreasing effect on the width between upper and lower control limits. For weak autocorrelation cases we expect the control limits to get narrower when it is compared with the strong autocorrelation. So the calculated values for $C^+_{RCCA(t)}$ and $C^-_{RCCA(t)}$ are expected to be smaller for strong autocorrelation to get larger control limits. As it can be observed from the formulations of $C^+_{RCCA(t)}$ and $C^-_{RCCA(t)}$ that are given in Equation (3.17), this can be provided by determining large $\hat{M}_o^t$ to get smaller $C^+_{RCCA(t)}$ values for strong autocorrelation and vice versa. By including the square of autocorrelation coefficient in the intercept, it is aimed to have larger (resp. smaller) target varying mean when observations are strongly autocorrelated (resp. weakly autocorrelated) in order to increase the correct signal rate.

While calculating $C^+_{RCCA(t)}$ and $C^-_{RCCA(t)}$, a slack value *k* is used to prevent the inclusion of small deviations from the process mean. In the relevant literature, *k* is

often chosen as a halfway between the target mean and the out-of-control value of the mean (Montgomery, 1997). It is important to select the right value for *k* since a large value of *k* will allow for large shifts in the mean without detection, while a small value of *k* will increase the frequency of false alarms. For a conventional CUSUM chart, *k* is selected to be equal to 0.5σ. During our comprehensive experiments, we observed that the RCCA gives better performance for $k=\frac{RCCAVP}{6}$. Calculations for D_o in Equation (3.18) are given in Table 3.11, below.

The reason for calculating $C^{+}_{RCCA(t)}$ and $C^{-}_{RCCA(t)}$ is similar to that of C^{+}_{t} (upper cumulative sum) and C^{-}_{t} (lower cumulative sum) statistics in CUSUM chart (Montgomery 1997). The basic purpose of a CUSUM chart is to track the distance between the actual data point and the grand mean. By keeping a cumulative sum of these distances, it can be determined if there is a change in the process mean. But, because $C^{+}_{RCCA(t)}$ and $C^{-}_{RCCA(t)}$ display some distinct characteristics from C^{+}_{t} and C^{-}_{t}, they are time dependent, and are not affected from their previous values, and we select the minimum value while calculating the $C^{-}_{RCCA(t)}$ (as depicted in Equation (3.17)), not the maximum value as in the calculation of C^{-}_{t} (Montgomery, 1997).

Step 5 Calculate the other parameters required for constructing the *RCCA*.

These parameters and the formulas used for calculations are given in Tables 3.11 through 3.14. As can be seen in Table 3.11 and Table 3.12, to calculate B, B_2, D_0; and B_3, B_4, L, D_1, D_3, D_4, and D_5, distinct formulas are employed due to the sign of $\hat{\beta}_0$ and of ϕ, respectively. On the other hand, signs of both $\hat{\beta}_0$ and ϕ determine which formulas will be used for D_2^{+} and D_2^{-}. As can be seen in Table 3.13, if $\phi > 0$, while deciding which formula will be used for D_2, magnitude of $\hat{\beta}_0$ is compared with $\phi RCCAVP$. According to our comprehensive experiments, the RCCA gives better performance in terms of false alarm rate with the parameters given in Tables

3.11 through 3.14, and the false alarm probability is lower when $\hat{\beta}_0$ and $\hat{\beta}_1$ have the same sign than when these parameters have opposite signs. Also big values of $\bar{C}^+$ increase the correct alarm rate for upward shift and vice versa. The magnitude and the sign of $\hat{\beta}_0$ directly affect the control chart performance. If the data have positive autocorrelation, unless the shift size is not changed, the performance gets better (worse) as the magnitude of positive $\hat{\beta}_0$ (negative $\hat{\beta}_0$) gets bigger, vice versa for negative autocorrelation. It is because the signs of $\hat{\beta}_0$ and ϕ affect the performance of the RCCA that Tables 3.11 through 3.14 are arranged in respect of the signs of these parameters. Because the RCCA has several parameters, the design procedure seems to be complicated. However, as can be seen in Tables 3.11-3.14, specifying values for some parameters can decrease the number of RCCA parameters and reduce the calculation complexity. Tables 3.11 - 3.14 show these special cases of the RCCA.

Table 3.11 Parameter calculations according to the sign of $\hat{\beta}_0$

If $\hat{\beta}_0 < 0$	**If $\hat{\beta}_0 \geq 0$**
$B_2^+ = 0 \quad B_2^- = 0$	$B_2^+ = 1 \quad B_2^- = 1$
$B^+ = \hat{\beta}_o + \left(\frac{EWMAARZ}{\bar{e}}\right)^2 \qquad B^- = -\hat{\beta}_o + \left(\frac{EWMAARZ}{\bar{e}}\right)^2$	$B^+ = 0 \quad B^- = 0$
$D_0 = -RCCAVP$	$D_0 = RCCAVP$

Table 3.12 Parameter calculations according to the sign of ϕ

If $\phi > 0$	If $\phi < 0$
$B_3^+ = 1 \quad B_3^- = 1$	$B_3^+ = \frac{\hat{\beta}_1}{\lvert\phi\rvert\lvert\hat{\beta}_0\rvert} \qquad B_3^- = \frac{\hat{\beta}_1}{\lvert\phi\rvert\lvert\hat{\beta}_0\rvert}$
$L = 3.0$	$L = 1.5$
$D_1 = 0 \;\; D_3 = 1 \;\; D_4 = 1 \;\; D_5 = 1$	$D_1 = \frac{1}{\lvert\phi\rvert} \;\; D_3 = 3L\phi^2 \;\; D_4 = -1.5 \;\; D_5 = \lvert\phi\rvert$
$B_4^+ = 1 \qquad B_4^- = 1$	$B_4^+ = \lvert\phi\rvert \qquad B_4^- = \lvert\phi\rvert$

Table 3.13 Parameter calculations for D_2 when $\phi > 0$

$\hat{\beta}_0 > 0$	$\hat{\beta}_0 > \phi$ *RCCAVP*	$D_2^+ = \frac{\hat{\beta}_0}{\phi(L/2)} + \frac{\hat{\beta}_0}{L(RCCAVP)}(L/2)\frac{\bar{C}^-}{\hat{\beta}_1}$
		$D_2^- = \frac{\hat{\beta}_0}{\phi(L/2)} + \frac{\hat{\beta}_0}{L(RCCAVP)}(L/2)\frac{\bar{C}^-}{\hat{\beta}_1} + 3\bar{C}^-\phi^2$
	$\hat{\beta}_0 \le \phi$ *RCCAVP*	$D_2^+ = \phi\hat{\beta}_0 + \phi^2 3L\bar{C}^- - (1/3)\bar{C}^+(1/\phi)$
		$D_2^- = \phi\hat{\beta}_0 + \phi^2 3L\bar{C}^- + (1/3)\bar{C}^+(1/\phi)$
$\hat{\beta}_0 \le 0$		$D_2^+ = \phi 2L(\bar{C}^- - \hat{\beta}_0)$
		$D_2^- = \phi 2L(\bar{C}^+ - \hat{\beta}_0)$

Table 3.14 Parameter calculations for D_2 when $\phi < 0$

$\hat{\beta}_0 > 0$	$D_2^+ = (-1/3)\frac{\hat{\beta}_0}{\phi^2} + (L)\left(\frac{\hat{\beta}_0}{L(RCCAVP)}\right)^2\left(\frac{\bar{C}^-\hat{\beta}_1}{\phi^2}\right) + \frac{\bar{C}^+}{\lvert\phi\rvert} - \frac{\bar{C}^-}{\phi^2}$
	$D_2^- = \frac{\hat{\beta}_0}{\lvert\phi\rvert} + (L)\left(\frac{\hat{\beta}_0}{L(RCCAVP)}\right)^2\left(\frac{\bar{C}^-\hat{\beta}_1}{\phi^2}\right) + 2\frac{\bar{C}^-}{\lvert\phi\rvert} - L\frac{\bar{C}^+}{\lvert\phi\rvert}$
$\hat{\beta}_0 \le 0$	$D_2^+ = \phi 2L(\bar{C}^- - \hat{\beta}_0)$
	$D_2^- = \phi 2L(\bar{C}^+ - \hat{\beta}_0)$

Step 6 Calculate control limits and the center line.

Control limits and the centre line of the RCCA are regression lines as given below.

Center line:

$$\hat{Y}_t = \hat{\beta}_0 + \hat{\beta}_1 t \tag{3.19}$$

Upper control limit (UCL):

$$UCL_t = Y_{UCLpre_t} + L(RCCAVP)\lvert\phi\rvert B_4^+ + D_2^+ - \frac{D_3 D_5^2 \bar{C}^+}{\phi^2} \tag{3.20}$$

where

$$Y_{UCLpre_t} = B^{+} + B_2^{+}\hat{\beta}_0 + D_1\left|\phi\right|\hat{\beta}_1\hat{\sigma} + B_3^{+}\left|\phi\right| EWMAARZ + \hat{\beta}_1 t \tag{3.21}$$

Lower control limit (LCL):

$$LCL_t = Y_{LCLpre_t} - L(RCCAVP)\left|\phi\right| B_4^{-} - D_2^{-} + \frac{D_4 D_5^2 \overline{C}^{-}}{\phi^2} \tag{3.22}$$

where

$$Y_{LCLpre_t} = -B^{-} - B_2^{-}\hat{\beta}_0 - D_1\left|\phi\right|\hat{\beta}_1\hat{\sigma} - B_3^{-}\left|\phi\right| EWMAARZ + \hat{\beta}_1 t \tag{3.23}$$

The simple linear regression equation with intercept ($\hat{\beta}_0$) and slope ($\hat{\beta}_1$) is used to represent the centre line of the RCCA. Also note that, if a relatively low observation from the autocorrelated process at the previous time step tends to be followed by another low value at the current time step, and a relatively large observation at the previous time step tends to be followed by another large value at the current time step, then this type of behavior is indicative of positive autocorrelation. Naturally, the direct contrary is indicative of negative autocorrelation. So the pattern on control chart varies according to the sign of the autocorrelation. To adjust control limits of the RCCA and consequently to provide a high correct signal rate, the calculations show disparities according to the combinations of the signs of intercept ($\hat{\beta}_0$) and autocorrelation coefficient (ϕ). For positive autocorrelation wider control limits are needed. The control limits' width should be narrower as the magnitude of positive autocorrelation coefficient decreases. For negative autocorrelation, control limits' width should be narrower with respect to the case of positive autocorrelation, and when strong negative autocorrelation exists it should be larger compared with the limits for weak negative autocorrelation. Control limits of the RCCA are also affected from the magnitude and the sign of $\hat{\beta}_0$.

To adjust continuously the distance between the center line and upper control limit due to the variations in observations that stem from the effect of autocorrelation, the parameters β_4^+ and L are employed. For a negative autocorrelation, with the effect of β_4^+, control limits get narrower while the autocorrelation decreases. If there is positive autocorrelation between process observations, then β_4^+ has no effect on control limits. Parameters D_2^+, D_3 and D_5 are also used to reflect the effect of deviations of observations from target varying mean with the combined effect of autocorrelation. The effect of D_2^+ on upper control limit varies according to the signs of $\hat{\beta}_0$ and ϕ. For a positive strong autocorrelation, if the sign of $\hat{\beta}_0$ is positive then the upper control limit will be wider than when $\hat{\beta}_0$ is negative. This effect begins to turn in direct contradiction with the decreasing autocorrelation between process observations. If there is a strong negative autocorrelation and if the sign of $\hat{\beta}_0$ is positive then the upper control limit will be narrower than when $\hat{\beta}_0$ is negative. The same effect continues for the decreasing negative autocorrelation from strong to weak with less impact. D_3 and D_5 decrease the width of upper control limit for negative autocorrelation since they have no impact on it for positive autocorrelation cases. Another parameter that is used for determining the width of upper control limit is $Y_{UCL\,\mathrm{Pr}\,e_t}$, which changes with respect to *t*. For $Y_{UCL\,\mathrm{Pr}\,e_t}$, by using parameters β^+ and β_2^+, the effect of smoothed standard deviation of the shifted process that depends on exponentially weighted residuals (EWMAARZ for RCCA) are taken into consideration. The sign of $\hat{\beta}_0$ affects the width of the control limits. This effect is reflected in the calculations of $Y_{UCL\,\mathrm{Pr}\,e_t}$ by β^+ and β_2^+. By considering the magnitude of $\hat{\beta}_0$ and exponentially weighted residuals, control charts' upper limit gets narrower for negative $\hat{\beta}_0$ values while it gets wider for positive values. By using D_1 and B_3^+, combined effect of autocorrelation and exponentially weighted residuals are added to the mathematical formulation of upper control limit. D_1 and B_3^+ show disparities according to the sign

of the autocorrelation coefficient ϕ. $Y_{UCL\,\mathrm{Pr}e_t}$ has an effect on determining the width of the upper control limit by reflecting the combined effect of exponentially weighted residuals as regards the signs of $\hat{\beta}_0$ and ϕ. The same approaches are employed in the calculations of the lower limit of the RCCA given in Equations (3.21-3.22).

3.3 Illustrative Example for the RCCA

Figure 3.7 and Figure 3.8 display the RCCA for 3.0σ and 0.5σ mean shifts, respectively. In these figures while the dashed line represents the shifted process, unshifted process is indicated by a solid line. To illustrate how this chart signals, the design procedure of the chart is computerized with MATLAB 7.4.0, and applied it to a sample of 500 observations generated using Equation (3.4). Design of the chart for these sample data was completed in 0.64s (less than 1s) of CPU time on a personal computer (AMD turion, 1.79 GHZ, 2.87 GB Ram). To model assignable causes, a shift is added in the mean of Z_t in (3.4) starting at observation 51. The parameter values employed for building the chart, degree of serial correlation, magnitudes of the mean shifts added to the 51st observation, and simulation results (the average number of points before an out-of-control signal is observed) are listed in Table 3.15. As can be seen in Figures 3.7 - 3.8, the chart gives out-of-control signals at time steps 11 and 19 after the mean shift occurs.

Table 3.15 Parameter values and the run length result for the illustrative example

Parameter	0.5σ	3.0σ
ϕ	0.95	0.95
L	3.0	3.0
$\hat{\beta}_1$	0.1768	0.1976
$\hat{\beta}_0$	6.9341	19.0294
X_1	10.2000	10.2000
$\bar{e}$	2.7054	3.6066
RCCAVP	6.6163	6.7144
$\bar{C}^+$	7.5301	15.9814
$\bar{C}^-$	3.9357	0.7747
EWMAARZ	5.0509	5.6830
Run length	19	11

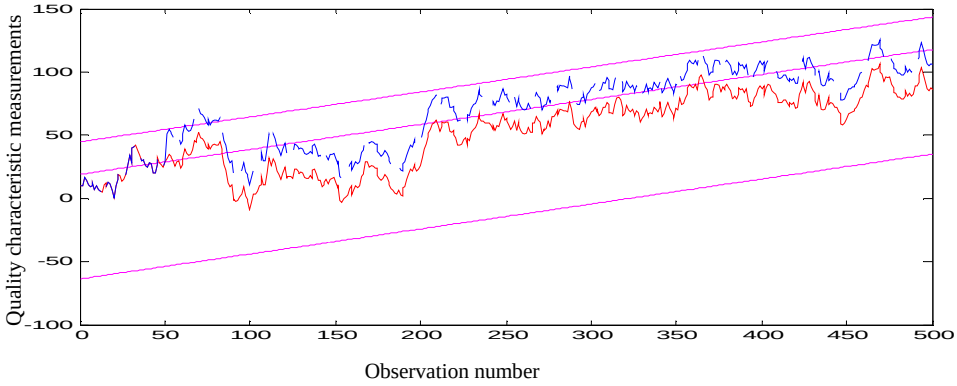

Figure 3.7 The RCCA for the 3.0σ shift.

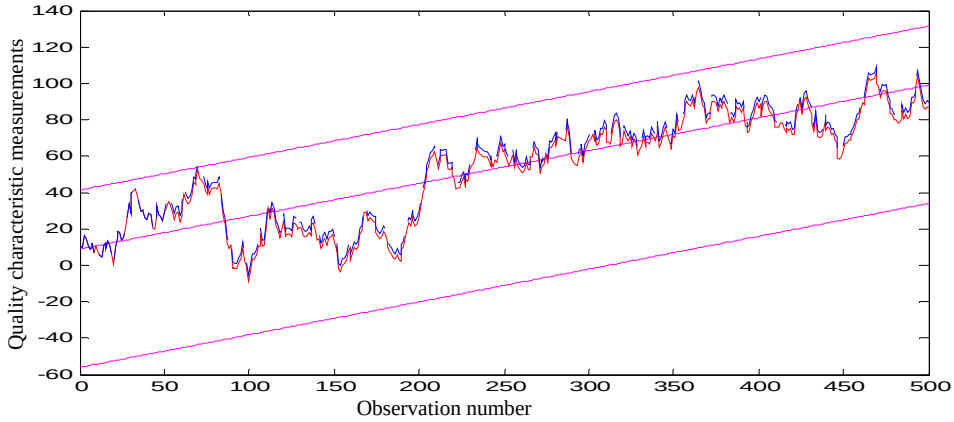

Figure 3.8 The RCCA for the 0.5σ shift.

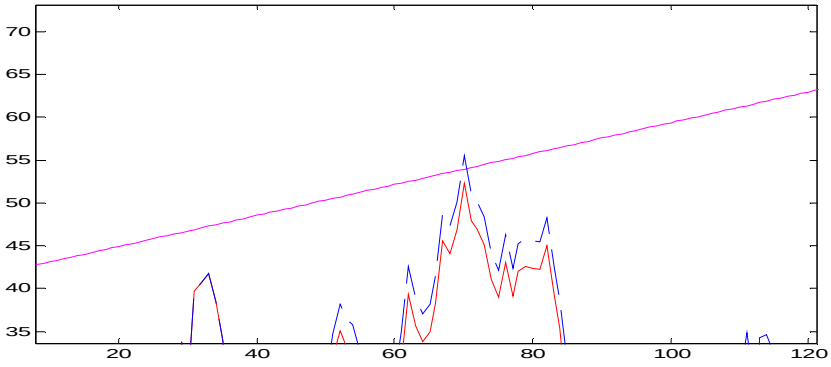

Figure 3.9 The RCCA for the 0.5σ shifted process data displayed in Figure 3.8 (widen image).

CHAPTER FOUR

PERFORMANCE EVALUATION OF THE PROPOSED CHART

The performance of control charts are measured via *average run length* (ARL). Essentially, the ARL is the average number of points that must be plotted before a point indicates an out-of-control condition. When there is a significant change in the process, it is desirable to have a low ARL so that the change will be detected quickly; when the process is in-control, it is desirable to have a large ARL so that the rate of false alarms produced by the chart is low (Lu & Reynolds, 1999). A desired control chart should have large in-control ARLs and small out-of-control ARLs (Winkel & Zhang, 2004). The presence of significant autocorrelation in the process observations can have a large impact on traditional control charts developed under the independence assumption. A typical effect of autocorrelation is to decrease the in-control average run length (ARL), which leads to a higher false alarm rate than in the case of independent observations, and to increase the time required to detect changes in the process. The ARL results indicate how fast, on average, the charts respond to process changes. However, these ARL results do not give a picture of the charts when actually applied to data. To provide a visual picture of different types of charts responding to various kinds of process changes, a basic set of simulated data, modified in specific ways to correspond to specific process changes, was used. In general, no single control chart will give optimal performance across a wide variety of situations. However, a control chart can be chosen to perform well for a particular type and magnitude of process change in an application (Lu & Reynolds, 1999). After the linear trend and serial correlation were diagnosed by means of NNs, the RCCA was used for different magnitudes of the mean shift, under the presence of various levels of autocorrelation. Performance of the RCCA was evaluated in terms of the average correct signal rate and the simulated average run length (ARL).

In this chapter, the average correct signal rate and the simulated average run length (ARL) performance of the RCCA are evaluated by using the following design parameters $\xi = 0$, $x_1 = 10$, $\varepsilon \sim N(0,4)$, N=500, and d=0.2. To investigate the performance, data sets are generated by using Equation (3.4), as we did in chapter three, and employing a wide range of possible shifts and autocorrelation coefficients. Each data set involves 500 observations. To model assignable causes, a sustained shift of magnitude δ_μ is induced in the mean of Z_t in Equation (3.4) starting at the 51st observation of the system. The considered shift magnitudes and autocorrelation coefficients are δ_μ = 0.0, 0.5, 1.0, 1.5, 2.0, 2.5, 3.0, and ϕ = 0.95, 0.475, -0.475, -0.95, respectively. For the sake of simplicity, we classified shift magnitudes in three groups as small (δ_μ = 0.5, 1.0), moderate (δ_μ = 1.5, 2.0), large (δ_μ = 2.5, 3.0), and autocorrelation coefficients as weak (ϕ = 0.475, -0.475) and strong (ϕ = 0.95, -095). For each data set 1000 simulation replications are performed. Simulation results are explained in detail below. If the test statistic of a shifted process does not fall between the control limits or the test statistic of an unshifted process falls between the control limits it is said that the control chart's signal is correct (Montgomery, 1997). In this context, the average correct signal rates for several shift-autocorrelation combinations are computed, which are displayed in Table 4.1. As can be seen from this table, signals of the chart are thoroughly accurate for all shift magnitudes in the presence of strong and weak negative autocorrelation. Its correct signal performance is also very good for large shift-positive autocorrelation combinations.

Table 4.1 Average correct signal rate

δ_μ \ ϕ	**(0.95)**	**(0.475)**	**(- 0.475)**	**(- 0.95)**
0.0	0.8310	0.9350	1.0000	0.9990
0.5	0.3475	0.5833	1.0000	0.9965
1.0	0.5101	0.7547	1.0000	0.9981
1.5	0.6159	0.8105	1.0000	0.9984
2.0	0.6876	0.8132	1.0000	0.9986
2.5	0.7388	0.8803	1.0000	0.9988
3.0	0.7675	0.9180	1.0000	0.9989

The simulated ARL performance of the RCCA is shown in Table 4.2. In this table, ARL for δ_μ=0.0 indicates ARL_0, in-control performance of the chart. It can be seen from Table 4.1 that the chart has large in-control ARL but small out-of-control ARL. That is, when the process has no mean shift the ARL is very large, and when a mean shift occurs the ARL decreases to indicate the occurrence of the mean shift quickly (Winkel & Zhang, 2004; Zhang, 2000). Consequently, we can say that the proposed chart has an ARL performance of what a desirable chart should have. About the overall ARL performance of the RCCA we can say that it performs well for large shifts, and shows its best ARL performance for negative autocorrelation cases. For moderate shifts its ARL performance is good for strong autocorrelation.

Table 4.2 ARL performance of the RCCA

δ_μ \ ϕ	**(0.95)**	**(0.475)**	**(- 0.475)**	**(- 0.95)**
0.0	388.3	411.4	449.0	449.0
0.5	46.6	212.6	449.0	57.5
1.0	34.3	182.1	165.3	22.9
1.5	13.7	41.7	17.9	12.6
2.0	9.6	36.4	4.4	7.1
2.5	3.2	8.1	1.7	3.6
3.0	1.2	3.6	1.1	1.1

According to the simulation results, the false alarm probability when β_0 and β_1 have the same sign is lower than when they have different signs. Also higher $\bar{C}^+$ increases the alarm rate for upward shift and vice versa. The magnitude and the sign of β_0 directly effects the control chart's performance. The performance of proposed chart increases for higher β_0 values for the same shift size when the positive autocorrelation occurs and vice versa for negative autocorrelation. The performance of proposed chart decreases for negative β_0 values. This experience is also valid for negative autocorrelation.

CHAPTER FIVE

CONCLUSION

In this thesis a new regression control chart that can be used to detect the shift in process having autocorrelated and trending data is proposed. This chart can handle data in which observations are both autocorrelated and their values linearly increase with respect to time. The standard assumptions that are usually cited in justifying the use of control charts are that the data generated by the in-control process are normally and independently distributed. However the independency assumption is not realistic in practice. Many processes such as those found in refinery operations, smelting operations, wood product manufacturing, waste-water processing and the operation of nuclear reactors have been shown to have autocorrelated observations. When there is significant autocorrelation in a process, traditional control charts with iid (independent and identically distributed) assumption can still be used, but they will be ineffective. These charts will result with poor performance like high false alarm rates and slow detection of process shifts.

On the other hand, if independent process data exhibit an underlying trend due to systemic causes, usually control charts based on ordinary least squares (OLS) regression are used for monitoring and control. Trends are usually due to gradual wearing out or deterioration of a tool or some other critical process components. In chemical processes linear trend often occurs because of settling or separation of the components of a mixture. They can also result from human causes, such as operator fatigue or the presence of supervision. Finally, trends can result from seasonal influences, such as temperature. The traditional control charts with horizontal control limits and a center line with a slope of zero have proven unreliable when systemic trend exists in process data. A device useful for monitoring and analyzing processes with trend is the regression control chart. However, since the Mandel's regression control chart was developed for independent data, it is not an effective tool for monitoring process shift in autocorrelated process observations.

In addition to autocorrelated or trended observations, many industrial processes give such data that exhibit both trend and autocorrelation among adjacent observations. In other words the types of industrial series (especially chemical processes) frequently exhibit a particular kind of trend behavior, that can be represented by a trend stationary first order autoregressive (trend AR(1)) model. Existing approaches may individually cope with autocorrelated and trending data. Although we made a comprehensive review, there appears to be no chart that monitors data which exhibit both increasing linear trend and serial correlation directly. This observation has been the motivation for the present dissertation on developing a new regression control chart (RCCA for short) that cope with autocorrelated observations in which observation values increase with respect to time.

Before presenting the proposed chart; the basic concepts of statistical process control charts, autocorrelation and time series models are described in chapter two. Also conventional regression control chart that is designed to control a varying (rather than a constant) average is discussed. Control charts for autocorrelated processes and conventional regression control chart were reviewed, and the historical progression in this field was emphasized.

In chapter three, the proposed regression control chart (RCCA) is presented. This chart requires the identification of trend AR(1) model as a suitable time series model for process observations. Therefore at first, autocorrelated and trending data set that corresponds with trend AR(1) process are generated. Then, to recognize trend in data, two LVQ and one MLP networks are combined, and then ENN is used to diagnose autocorrelation through the trended data. When the literature is reviewed, it is observed that there is not any combined neural network structure that combines LVQ, MLP and ENN networks together to recognize the autocorrelated and trended patterns. Different statistical tools (such as least squares for trend analysis and time series analysis for calculating autocorrelation coefficients) can be easily implemented to process data to recognize the trend or autocorrelation in process data but when compared to other methodologies the neural network approach has certain

advantages. First of all, the model development is much simpler than that for most other approaches. Instead of theoretical analysis and development for a new model the neural network tailors itself to the training data. The model can be refined at any time with the addition of new training data. After recognizing autocorrelated and trending data by the means of proposed neural network structure, proposed regression control chart (RCCA) is applied to the data and its operating characteristics are experimented. The construction steps of RCCA to detect shift in autocorrelated and trending process observations is overviewed with an illustrative example.

The average correct signal rate and the ARL performance of the chart are investigated by simulation approach in chapter four. Based on the results of simulation, it is safe to say that the RCCA is a considerably powerful chart. As it is known, no single control chart will give optimal performance across a wide variety of situations. In this sense, we tried to explain when the proposed control chart performs well for several types of autocorrelation structures and shift magnitudes. The proposed control chart produces desirable results under given assumptions and parameter design.

It is well known that the same two designs using the same chart parameters based on two different input sets may produce very different chart performance. The proposed chart gives good ARL results; all their results are based on an assumption that the regression model relating the process output and the external covariate(s) is exactly known. In practice, the regression model parameter estimation, sign of the estimated parameters, starting value of the independent variable, the observation number that shift in process mean occurred, and the direction of shift may seriously affect the charting performance of proposed regression control chart for autocorrelated data.

As it is known, a traditional residual chart takes into account only the current sample when determining the status of a process and hence does not provide any pattern-related information. By using the RCCA practitioners will be able to monitor

current samples of an autocorrelated and trending process directly and to observe the progress of the process. Practitioners can easily computerize and directly apply this chart to original data. This study could be extended for autocorrelated data with decreasing trend.

REFERENCES

Al-Assaf, Y. (2004). Recognition of control chart patterns using multi-resolution wavelets analysis and neural networks. *Computers & Industrial Engineering, 47* (1), 17-29.

Alwan, L. C., & Roberts, H. V. (1988). Time series modeling for statistical process control. *Journal of Business and Economic Statistics, 6* (1), 86-95.

Anagun, A.S. (1998). A neural network applied to pattern recognition in statistical process control. *Computers & Industrial Engineering, 35* (1-2), 185-188.

Apley, D. W., & Shi, J. (1999). The GRLT for statistical process control of autocorrelated processes. *IIE Transactions, 31*, 1123-1134.

Asadzadeh, S., Aghaie, A., & Shahriari, H. (2009). Monitoring dependent process steps using robust cause-selecting control charts. *Quality and Reliability Engineering International, 25* (7), 851-874.

Atienza, L. C., Tang, L. C., & Ang, B. W. (1997). ARL properties of a sample autocorrelation chart. *Computers & Industrial Engineering, 33* (3-4), 733-736.

Ben-Gal, I., Morag, G., & Shmilovici, A. (2003). Context-based statistical process control: A monitoring procedure for state-dependent processes. *Technometrics, 45* (4), 293-311.

Brence, J. R., & Mastrangelo, C. M. (2006). Parameter selection for a robust tracking signal. *Quality and Reliability Engineering International, 22* (4), 493-502.

Besterfield, D. H., Besterfield-Michna, C., Besterfield, G. H., & Besterfield-Sacre, M. (2003). *Total quality Management* (3rd ed.). NJ: Prentice-Hall.

Box, G. E. P., & Jenkins, G. M (1976). *Time series analysis - forecasting and control* (1st ed.). California: Holden-Day Inc.

Box, G., & Ramirez, J. (1992). Cumulative score charts. *Quality and Reliability Engineering International, 8* (11), 17-27.

Castillo, E. D., & Montgomery, D. C. (1994). Short-run statistical process control: Q-chart enhancements and alternative methods. *Quality and Reliability Engineering International, 10* (2), 87-97.

Cheng, C. S. (1997). A neural network approach for the analysis of control chart patterns. *International Journal of Production Research, 35* (3), 667-697.

Cheng, J. C., & Chou, C. Y. (2008). A real-time inventory decision system using Western Electric run rules and ARMA control chart. *Expert Systems with Applications*, *35* (3), 755-761.

Chiu, C. C., Chen, M. K., & Lee, K. M. (2001). Shift recognition in correlated process data using a neural network. *International Journal of System Science, 32* (2), 137-143.

Costa, A. F. B., & Claro, F. A. E. (2008). Double sampling $\bar{X}$ control chart for a first-order autoregressive moving average process model. *International Journal of Advanced Manufacturing Technology*, *39* (5-6), 521-542.

Eleni, S., Demetrios, K., & Leonidas, K., (2005). Statistical process techniques on water toxicity data. Retrieved September 27, 2007, from http://www.aueb.gr /pympe/hercma/proceedings2005/H05-FULL-PAPERS-1/H05-WORDPAPERS/ hercma-2005-smeti-koronakis-kousouris.doc.

Gauri, S. K., & Chakraborty, S. (2006). Feature-based recognition of control chart patterns. *Computers & Industrial Engineering*, *51* (4), 726-742.

Gauri, S. K., & Chakraborty, S. (2008). Improved recognition of control chart patterns using artificial neural networks. *International Journal of Advanced Manufacturing Technology, 36* (11-12), 1191-1201.

Gauri, S. K., & Chakraborty, S. (2009). Recognition of control chart patterns using improved selection of features. *Computers & Industrial Engineering, 56* (4), 1577-1588.

Ghourabi, M., & Limam, M. (2007). Residual responses to change patterns of autocorrelated processes. *Journal of Applied Statistics, 34* (7), 785-798.

Guh, R.S., & Tannock, J.D.T. (1999). Recognition of control chart concurrent patterns using a neural network approach. *International Journal of Production Research, 37* (8), 1743-1765.

Guh, R. S. (2008). Real-time recognition of control chart patterns in autocorrelated processes using a learning vector quantization network-based approach. *International Journal of Production Research, 46* (14), 3959-3991.

Ham, F. M., & Kostanic, I. (2001). *Principles of neurocomputing for science and engineering* (1st ed.). NY: McGraw-Hill.

Harris, T. J., & Ross, W. H. (1991). Statistical process-control procedures for correlated observations. *Canadian Journal of Chemical Engineering, 69* (1), 48-57.

Hawkins, D. M. (1991). Multivariate quality control based on regression-adjusted variables. *Technometrics, 33* (1), 61-75.

Haworth, D. A. (1996). Regression control charts to manage software maintenance. *Journal of Software Maintenance-Research and Practice, 8* (1), 35-48.

Hwarng, H. B., & Hubele, N. F. (1993). Backpropagation pattern recognizers for (x)over-bar control charts-methodology and performance. *Computers & Industrial Engineering, 24* (2), 219-235.

Hwarng, H.B., & Wang, Y., (2010). Shift detection and source identification in multivariate autocorrelated processes. *International Journal of Production Research*, 48 (3), 835-859.

Issam, B. K., & Mohamed, L. (2008). Support vector regression based residual MCUSUM control chart for autocorrelated process. *Applied Mathematics and Computation*, *201* (1-2), 565-574.

Jiang, W. (2001). Average run length computation of ARMA charts for stationary processes. *Communications in Statistics-Simulation and Computation, 30* (3), 699-716.

Jiang, P. Y., Liu, D. Y., & Zeng, Z. J. (2009). Recognizing control chart patterns with neural network and numerical fitting, *Journal of Intelligent Manufacturing, 20* (6), 625-635.

Jiang, W., Tsui, K. L., & Woodal, W. H. (2000). A new SPC monitoring Method: The ARMA Chart. *Technometrics, 42* (4), 399-410.

Jiang, W., Wu, H., Tsung, F., Nair V., & Tsui, K. L., (2002). PID Charts for Process Monitoring. *Technometrics, 44* (3), 205-214.

Johnson, R. A., & Bagshaw, M. (1974). The effect of serial correlation on the performance of CUSUM tests. *Technometrics*, *16* (1), 103-112.

Kacker, R., & Zhang, N. F. (2002). Online control using integrated moving average model for manufacturing errors. *International Journal of Production Research, 40* (16), 4131-4146.

Kalagonda, A. A., & Kulkarni, S. R. (2003). Diagnosis of multivariate control chart signal based on dummy variable regression technique. *Communications in Statistics-Theory and Methods, 32* (8), 1665-1684.

Kim, S. H., Alexopoulos, C., Goldsman, D., & Tsui, K. L. (2006). A new model-free CUSUM procedure for autocorrelated processes. Technical report, School of Industrial and Systems Engineering, Georgia Institute of Technology, Atlanta, GA. Retrieved November 12, 2007, from http://www2.isye.gatech.edu/~skim/ MFC.pdf.

Kim, S. H., Alexopoulos, C., Tsui, K. L., & Wilson, J. R. (2007). A distribution - free tabular CUSUM chart for autocorrelated data. *IEE Transactions*, *39* (3), 317-330.

Koksal, G., Kantar, B., & Ula, T. A. (2008). The effect of Phase I sample size on the run length performance of control charts for autocorrelated data. *Journal of Applied Statistics*, *35* (1), 67-87.

Knoth, S., Morais, M.C., Pacheco, A., & Schmid, W., (2009). Misleading Signals in Simultaneous Residual Schemes for the Mean and Variance of a Stationary Process. *Communications in Statistics-Theory and Methods*, 38 (16-17), 2923-2943.

Kramer, H., & Schmid, W. (1997). Control charts for time series. *Nonlinnear Analysis, Theory, Methods & Applications*, *30* (7), 4007-4016.

Kudo, T. Y. (2001). *Using statistical process control methods to classify pilot mental workload*. Retrieved November 12, 2007, from https://research.maxwell. af.mil/papers/ ay2001/afit/afit-gor-ens-01m-10.pdf.

Lee, S.W., & Song, H.H. (1997) A new recurrent neural-network architecture for visual pattern recognition. *IEEE Transactions on Neural Networks*, 8 (2), 331-339.

Levine, D. M., Ramsey, P. P., & Berenson, M. L. (1995). *Business Statistics for Quality and Productivity* (1st ed.). NJ: Prentice-Hall.

Longnecker, M. T., & Ryan, T. P. (1992). Charting correlated process data (Technical Report 166). *Texas A&M University, Department of Statistics*.

Lowry, C. A., & Montgomery, D. C. (1995). A review of multivariate control charts. *IEE Transactions, 27* (6), 800-810.

Lu, C. W., & Reynolds, M. R. (1999). EWMA control charts for monitoring the mean of autocorrelated processes. *Journal of Quality Technology, 31* (2), 166-188.

Lucas, J., & Saccucci, M. S. (1990). Exponentially weighted moving average control schemes, properties and enhancements. *Technometrics, 32* (1), 1-12.

Luceno, A., & Box, G. E. P. (2000). Influence of the sampling interval, decision limit and autocorrelation on the average run length in CUSUM charts. *Journal of Applied Statistics, 27* (2), 177-183.

Mandel, J. (1969). The regression control chart. *Journal of Quality Technology, 1* (1), 1-6.

Manuele, J. (1945). Control chart for determining tool wear. *Industrial Quality Control, 1,* 7-10.

Mastrangelo, C. M., & Montgomery, D. C. (1995). SPC with correlated observations for the chemical and process industries. *Quality and Reliability Engineering International, 11* (2), 79-89.

Mills, T. C. (1990). *Time series techniques for economists* (1st ed.). Cambridge: Cambridge University Pres.

Montgomery, D. C., (1997). *Introduction to statistical quality control* (3rd ed.). NY: John Wiley & Sons, Inc.

Montgomery, D. C. (2009). *Statistical Quality Control: A Modern Introduction* (6th ed.) Hoboken, NJ: John Wiley & Sons, Inc.

Montgomery, D. C., & Johnson, L. A. (1976). *Forecasting and time series analysis* (1st ed.). NY: McGraw- Hill.

Montgomery, D. C., & Mastrangelo, C. M. (1991). Some statistical process control methods for autocorrelated data. *Journal of Quality Technology, 23* (3), 179-193.

Montgomery, D. C., & Runger, G. C. (1999). *Applied statistics and probability for engineers* (2nd ed.). NY: John Wiley & Sons, Inc.

Nembhard, H. B., Mastrangelo, C. M., & Kao, M. S. (2001). Statistical monitoring performance for startup operations in a feedback control system. *Quality and Reliability Engineering International, 17* (5), 379-390.

Noorossana, R., & Vaghefi, S. J. M. (2006). Effect of autocorrelation on performance of the MCUSUM control chart. *Quality and Reliability Engineering International, 22* (2), 191-197.

Oakland, J. S., (2003). *Statistical process control* (5th Ed.). Amsterdam: Butterworth & Heinemann.

Omura, A. P., & Steffe, J. F. (2003). Mixer viscometry to characterize fluid foods with large particulates. *Journal of Food Process Engineering, 26* (5), 435-445.

Oztemel, E. (2003). *Artificial Neural Networks* (1st ed.). Istanbul: Papatya press.

Pacella, M., & Semeraro, Q. (2007). Using recurrent neural networks to detect changes in autocorrelated processes for quality monitoring. *Computers & Industrial Engineering, 52* (4), 502-520.

Pham, D. T., & Chan, A. B. (2001). Unsupervised adaptive resonance theory neural networks for control chart pattern recognition. *Proceedings of the Institution of Mechanical Engineers Part B-Journal of Engineering Manufacture, 215* (1), 59-67.

Pham, D. T., & Oztemel, E. (1992a). Control chart pattern recognition using neural Networks. *Journal of Systems Engineering, 2* (4), 256-262.

Pham, D. T., & Oztemel, E. (1994). Control chart pattern recognition using Learning vector quantization networks. *International Journal of Production Research, 32* (3), 721729.

Pham, D. T., & Sagiroglu, S. (2001). Training multilayered perceptrons for pattern recognition: a comparative study of four training algorithms. *International Journal of Machine Tools & Manufacture, 41* (3), 419-430.

Quesenberry, C. P. (1988). A SPC approach to compensating a tool-wear process. *Journal of Quality Technology, 20* (4), 220-229.

Rao, B. V., Disney, R. L., & Pignatiello, J. J. (2001). Uniqueness and converges of solutions to average run length integral equations for cumulative sum and other control charts. *IEE Transactions, 33* (6), 463-469.

Reynolds, M. R., & Lu, C. W. (1997). Control charts for monitoring processes with autocorrelated data. *Nonlinear Analysis, Theory, Methods & Applications, 30* (7), 4059-4067.

Ross, J. E. (1999). *Total quality management* (3rd ed.). NY: St. Lucie Press.

Runger, G. C., & Willemain, T. R. (1995). Model-based and model-free control of autocorrelated processes. *Journal of Quality Technology, 27* (4), 283-292.

Russell, R. S., & Taylor, B. W. (1998). *Operations management* (2nd ed.). NJ: Prentice-Hall.

Samanta, B., & Bhattacherjee, A. (2001). An investigation of quality control charts for autocorrelated data. *Mineral Resources Engineering, 10* (1), 53-69.

Sheu, S. H., & Lu, S. L. (2009). Monitoring the mean of autocorrelated observations with one generally weighted moving average control chart. *Journal of Statistical Computation and Simulation, 79* (12), 1393-1406.

Shu, L., & Tsung, F. (2000). Multistage process monitoring and diagnosis. *Management of innovation and technology, 2000, ICMIT 2000, Proceedings of the 2000 IEEE international conference on, 1*, 881-886.

Shu, L., Apley, D. W., & Tsung, F. (2002). Autocorrelated process monitoring using triggered cuscore charts. *Quality and Reliability Engineering International, 18* (5), 411-421.

Shu, L., Tsung, F., & Kapur, K. C. (2004). Design of multiple cause-selecting charts for multistage processes with model uncertainty. *Quality Engineering, 16* (3), 437 - 450.

Shu, L., Tsung, F. & Tsui, K. L. (2004). Run-length performance of regression control charts with estimated parameters. *Journal of Quality Technology, 36* (3), pp. 280-293.

Shu, L., Tsung, F., & Tsui, K. L. (2005). Effects of estimation errors on cause-selecting charts. *IEEE Transactions, 37* (3), 559-567.

Snoussi, A., Ghourabi, M. E., & Limam, M. (2005). On spc for short run autocorrelated data. *Communications in Statistics-Simulation and Computation, 34* (1), 219-234.

Sulek, J. M., Marucheck, A., & Lind M. R. (2006). Measuring performance in multi-stage service operations: An application of cause selecting control charts. *Journal of Operations Management, 24* (5), 711-727.

Swift, J. A., Ross, J. E., & Omachonu, V. K. (1998). *Principles of total quality* (2nd ed.). Boca Raton, Florida: St. Lucie Press.

Tanya, R. (1999). *A Guide To The Methodological Foundations of Quality Oversight and Improvement Processes*. Retrieved December 22, 2006, from http://www.edb.utexas.edu/faculty/fouladi/quality.pdf.

Triantafyllopoulos, K. (2006). Multivariate control charts based on Bayesian state space models. *Quality and Reliability Engineering International*, *22* (6), 693-707.

Utley, J. S., & May, J. G. (2008). Residual control charts and LAV regression. *39th Annual Meeting of the Decision Sciences Institute,* 3521-3526.

Utley, J. S., & May, J. G. (2009). Monitoring service quality with residual control charts. *Managing Service Quality*, *19* (2), 162-178.

Wade, M. R, & Woodall, W. H. (1993). A review and analysis of cause selecting control charts. *Journal of Quality Technology*, *25* (3), 161-170.

Wang, C. H., Dong, T. P., & Kuo, W. (2009). A hybrid approach for identification of concurrent control chart patterns. *Journal of Intelligent Manufacturing, 20* (4), 409-419.

Wardell, D. G., Moskowitz, H., & Plante, R. D. (1992). Control chart in the presence of data correlation. *Management Science, 38* (8), 1084-1105.

Wardell, D. G., Moskowitz, H., & Plante, R. D. (1994). Run-length distribution of special-cause control charts for correlated processes. *Technometrics, 36* (1), 3-17.

Weiss, C. H., & Testik, M. C. (2009). CUSUM Monitoring of First-Order Integer-Valued Autoregressive Processes of Poisson Counts. *Journal of Quality Technology*, *41* (4), 389-400.

West, D.A., Mangiameli, P.M., & Chen, S.K. (1999). Control of complex manufacturing processes: a comparison of SPC methods with a radial basis function neural network. *Omega-International Journal of Management Science***,** 27 (3), 349-362.

Wetherill, G. B, & Brown, D. W (1991). *Statistical process control: theory and practice* (1st ed.). London: Chapman & Hall.

Willemain, T. R, & Runger G. C. (1998). Statistical process control using run sums. *Journal of Statistical Computation and Simulation, 61* (4), 361-378.

Winkel, P., & Zhang, N. F. (2004). Serial correlation of quality control data-on the use of proper control charts. *Scandinavian Journal of Clinical and Laboratory Investigation, 64* (3), 195-204.

Winkel, P., & Zhang, N. F. (2005). Effect of uncertainty components such as recalibration on the performance of quality control charts. *Scandinavian Journal of Clinical and Laboratory Investigation, 65* (8), 707-720.

Yang, S. F. (2005). Dependent processes control for overadjusted process means. *International Journal of Advanced Manufacturing Technology, 26* (1-2), 109-116.

Yang, S. F., & Chen, W. Y. (2009). Controlling over-adjusted process means and variances using VSI cause selecting control charts. *Expert Systems with Applications, 36* (3), 7170-7182, Part 2.

Yang, J., & Makis, V. (1997). On the performance of classical control charts applied to process residuals. *Computers & Industrial Engineering, 33* (1-2), 121-124.

Yang, S. F., & Su, H. C. (2007). Adaptive sampling interval cause-selecting control charts. *International Journal of Advanced Manufacturing Technology, 31* (11-12), 1169-1180.

Yang, S. F., & Yang, C. M. (2005). Effects of imprecise measurement on the two dependent processes control for the autocorrelated observations. *International Journal of Advanced Manufacturing Technology, 26* (5), 623-630.

Yang, C. M., & Yang, S. F. (2006). Optimal control policy for dependent process steps with over-adjusted means and variances. *International Journal of Advanced Manufacturing Technology, 29* (7-8), 758-765.

Yang, S. F., & Yang, C. M. (2006). An approach to controlling two dependent process steps with autocorrelated observations. *International Journal of Advanced Manufacturing Technology, 29* (1-2), 170-177.

Yourstone, S. A., & Montgomery D. C. (1989). A time-series approach to discrete real-time process quality control. *Quality and Reliability Engineering International, 5* (4), 309-317.

Yourstone, S. A., & Montgomery, D. C. (1991). Detection of process upsets-sample autocorrelation control chart and group autocorrelation control chart applications. *Quality and Reliability Engineering International, 7* (3), 133-140.

Zhang, G. X. (1984). A new type of control charts and theory of diagnosis with control charts. *World Quality Congress Transactions, American Society for Quality Control: Milwaukee, WI*, 175-185.

Zhang, N. F. (1997). Detection capability of residual control chart for stationary process data. *Journal of Applied Statistics, 24* (4), 475-492.

Zhang, N. F. (1998). A statistical control chart for stationary process data. *Technometrics, 40* (1), 24-38.

Zhang, N. F. (2000). Statistical control charts for monitoring the mean of a stationary process. *Journal of Statistical Computation Simulation, 66* (3), 249-258.

Zou, C., Wang, Z., & Tsung, F. (2008). Monitoring autocorrelated processes using variable sampling schemes at fixed-times. *Quality and Reliability Engineering International, 24* (1), 55-69.

APPENDICES

Appendix 1. The Process Simulator

The process simulator for generating the uncorrelated CCP examples is given below in Equations (A1.1 - A1.5) (Oztemel, 2003):

Pattern formulation of normal distribution:

$$y_t = \mu + r_t \sigma \tag{A1.1}$$

$$r_t = \sqrt{-2\ln(u)\cos 2\pi u} \tag{A1.2}$$

where u is uniform [0,1] random variable, t is the observation number (or time step), and π is the Pi constant.

Pattern formulations of increasing or decreasing trend:

$$y_t = \mu + r_t \sigma \mp gt \tag{A1.3}$$

where g is the trend slope of uncorrelated process.

Pattern formulation of sliding up or sliding down:

$$y_t = \mu + r_t \sigma \mp k_{sliding} s_{displacement} \tag{A1.4}$$

where $k_{sliding}$ is the sliding coefficient at the sliding moment, and the $s_{displacement}$ is the displacement of process mean in terms of standard deviation.

Pattern formulation of periodic shifting:

$$y_t = \mu + r_t \sigma + \alpha_{periodic} \sin(2\pi t / N) \tag{A1.5}$$

where $\alpha_{periodic}$ is the dimension of the periodic shifting (random integer variable), and N is the number of observations.

The process simulator for generating the CCP examples in the AR(1) process is given below at Equations (A1.6 - A1.11) (Guh, 2008):

$$x_t = \xi + \phi_1 x_{t-1} + \varepsilon_t \tag{A1.6}$$

$$X_t = x_t + d_t \tag{A1.7}$$

where d_t is the special disturbance at time t (zero when no unnatural pattern present).

Pattern formulation of normal distribution:

$$d_t = 0 \tag{A1.8}$$

Pattern formulations of increasing or decreasing trend:

$$d_t = \pm dt \tag{A1.9}$$

where d is the trend slope of autocorrelated process.

Pattern formulation of sliding up or sliding down:

$$d_t = \pm k_{sliding} s_{displacement} \tag{A1.10}$$

Pattern formulation of periodic shifting:

$$d_t = \alpha_{periodic} \sin(2\pi t / N) \tag{A1.11}$$

Appendix 2. Learning Rules of the MLP NN

MLP learns by generalized form of Delta learning rule which depends on least squares method. Delta rule composed of two phases. The first phase is 'feedforward' and the second phase is 'back propagation'. In the first phase the output of the NN is calculated and in the second phase, the weights of arcs are recalculated to minimize the error term.

Phase I: The data processing is started with presenting an input to the NN from input layer. There is no data processing in the input layer so the inputs are sent to hidden layer without changing. The output of *k*th process element y_k in input layer is calculated by the formula given in Equation (A2.1):

$$y_k = I_k \tag{A2.1}$$

where I_k is the input for *k*th process element of input layer. Each process element in the hidden layer gets the information from input layer by the effect of connection weights. The net input that comes to process elements of hidden layer (u_j) is calculated by:

$$u_j = \sum_{k=1}^{N} w_{kj} y_k \tag{A2.2}$$

where w_{kj} is the weight between *k*th input layer process element and *j*th hidden layer process element. Output of any neuron that is represented by u_q is calculated by using one of the transfer functions that are given in Table A2.1.

Table A2.1. Activation functions

Activation function	Formula	Activation function	Formula
Sigmoid function	$F(u_q) = \frac{1}{1+e^{-u_q}}$	Sinus function	$F(u_q) = Sin(u_q)$
Linear function	$F(u_q) = u_q$	Threshold value function	$F(u_q) = \begin{cases} 0 \ if \ \ u_q \le 0 \\ u_q \ \ if \ \ 0 < u_q < 1 \\ 1 \ else \end{cases}$
Step function	$F(u_q) = \begin{cases} 1 \ if \ \ u_q > threshold(\theta_q) \\ 0 \ else \end{cases}$	Hyperbolic tangent function	$F(u_q) = \frac{e^{u_q} + e^{-u_q}}{e^{u_q} - e^{-u_q}}$

Phase II: The output of the network for the given input is compared with the expected value of the network's output. Because of the expected value of the output for each input that is represented to the network is known, MLP is known as a supervised learning algorithm. The error for *m*th process element in the output layer is calculated by:

$$e_m = E[y_m] - y_m \tag{A2.3}$$

where $E[y_m]$ is the expected output and e_m is the error occured at the output of *m*th process element. This error term is multiplied by the differention of output value and by this way the error ratios (δ) that will be distributed to weights are determined. The δ that will be distributed to weights for the *m*th process element is calculated by the formula given in Equation (A2.4)

$$\delta_m = f'(u) e_m \tag{A2.4}$$

If the output function is sigmoid than the δ that will be distributed to weights for the *m*th process element is

$$\delta_m = y_m (1 - y_m) e_m \tag{A2.5}$$

where $y_m(1-y_m)$ is the differention of sigmoid function. If the amount of change for the weights between hidden layer and output layer are calculating than the δ will be:

$$\delta_j = f'(u)\sum_m \delta_m w_{jm} \tag{A2.6}$$

The amount of change for weights at *t*th iteration is:

$$\Delta w_{jm}(t) = \lambda \delta_m y_j + \alpha \Delta w_{jm}(t-1) \tag{A2.7}$$

where $\Delta w_{jm}(t)$ is the amount of change for the weight between *j*th process element of hidden layer and *m*th process element of output layer at time *t* (or *t*th iteration), λ is the learning rate, and α is the momentum coefficient. Note that, the momentum coefficient (α) provides the neural network not to delay on a local optimum point (Oztemel, 2003). After calculating the amount of change, the new values of the weights at *t*th iteration is:

$$w_{jm}(t) = w_{jm}(t-1) + \Delta w_{jm}(t) \tag{A2.8}$$

Other weights for other layers are calculated by the same way. Similarly the weights of the threshold unit have to be modified. The output of this unit is fixed and equal to 1. So the amounts of changes for the weights of threshold unit of the process element at the output layer are

$$\Delta b_m(t) = \lambda \delta_m + \alpha \Delta b_m(t-1) \tag{A2.9}$$

After calculating the amount of change, the new values of the weights at *t*th iteration is:

$$b_m(t) = b_m(t-1) + \Delta b_m(t) \tag{A2.10}$$

where $b_m(t)$ is the new value of the weight between threshold unit and *m*th process element of output layer. The other weights are calculated by the same way. Figure A2.1 displays a sample network topology for a backpropogation network. For the sake of simplicity, a MLP network with two hidden layers is derived.

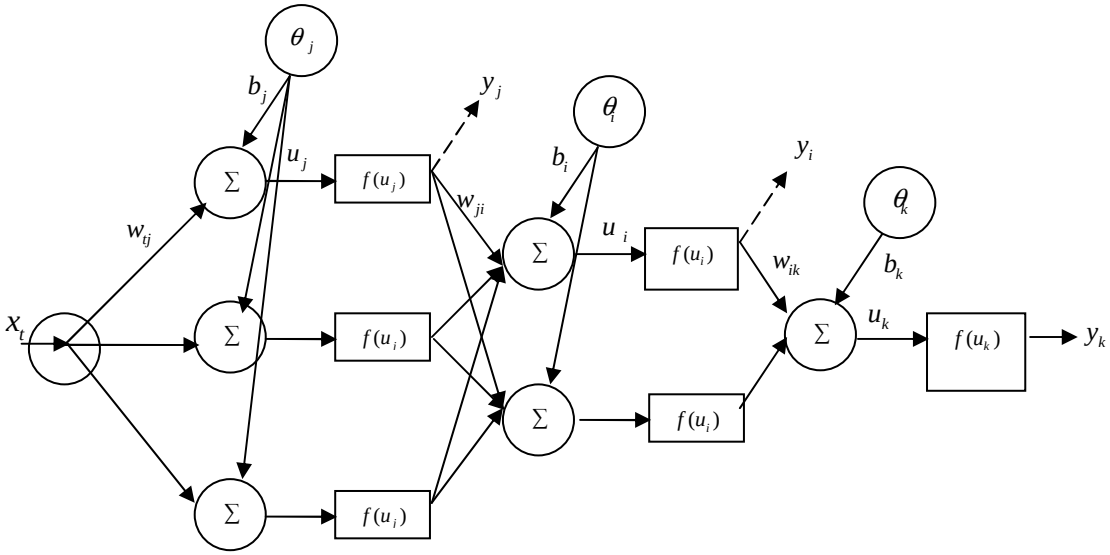

Figure A2.1. A sample MLP architecture for the given data set.

The notation is given below:

b_i, b_j, b_k : Weights for threshold values

w_{ik}, w_{ji}, w_{tj} : Weights for the neurons

y_i, y_j, y_k : Outputs of the transformation functions

u_i, u_j, u_k : Total entries to the neurons

The formulation is given below:

$$\mathrm{E}=\frac{1}{2}\sum_k e_k^2 \qquad \text{(A2.11)}$$

$$e_k = E[y_k] - y_k \qquad \text{(A2.12)}$$

for θ_q=1

$$\text{Feedforward 1: } y_j = f(u_j) \text{ and } u_j = \left(\sum_t w_{tj} x_t\right) + \theta_j b_j \qquad \text{(A2.13)}$$

Feedforward 2: $y_i = f(u_i)$ and $u_i = \left(\sum_j w_{ji} y_j \right) + \theta_i b_i$ (A2.14)

Feedforward 3: $y_k = f(u_k)$ and $u_k = \left(\sum_i w_{ik} y_i \right) + \theta_k b_k$ (A2.15)

For sigmoid functions $f(u) = \frac{1}{1+e^{-u}}$ and $f(u)' = f(u)(1-f(u))$ (A2.16)

Back Propagation 1:

$$\frac{\partial E}{\partial w_{ik}} = \frac{\partial E}{\partial e_k}\frac{\partial e_k}{\partial y_k}\frac{\partial y_k}{\partial u_k}\frac{\partial u_k}{\partial w_{ik}} = e_k(-1) f'(u_k) y_i \quad \text{(A2.17)}$$

$$\delta = f(u)(1-f(u))e \quad \text{(A2.18)}$$

$$\delta_k = e_k f'(u_k) \quad \text{(A2.19)}$$

$$\frac{\partial E}{\partial w_{ik}} = e_k(-1) f'(u_k) y_i = -\delta_k y_i \quad \text{(A2.20)}$$

$$\Delta w_{ik} = -\lambda \frac{\partial E}{\partial w_{ik}} = +\lambda \delta_k y_i \quad \text{(A2.21)}$$

If the momentum coefficient is used not to delay on a local optimum:

$$\Delta w_{ik}(t) = \lambda \delta_k y_i + \alpha \Delta w_{ik}(t-1) \quad \text{(A2.22)}$$

$$\frac{\partial E}{\partial b_k} = \frac{\partial E}{\partial e_k}\frac{\partial e_k}{\partial y_k}\frac{\partial y_k}{\partial u_k}\frac{\partial u_k}{\partial b_k} = e_k(-1) f'(u_k)(+1) \quad \text{(A2.23)}$$

$$\frac{\partial E}{\partial b_k} = -e_k f'(u_k) = -\delta_k \quad \text{(A2.24)}$$

$$\Delta b_k = -\lambda \frac{\partial E}{\partial b_k} = +\lambda \delta_k \quad \text{(A2.25)}$$

if the momentum coefficient is used not to delay on a local optimum:

$$\Delta b_k(t) = \lambda \delta_k + \alpha \Delta b_k(t-1) \quad \text{(A2.26)}$$

$$w_{ik}(new) = w_{ik}(old) + \Delta w_{ik} \quad \text{(A2.27)}$$

$$b_k(new) = b_k(old) + \Delta b_k \quad \text{(A2.28)}$$

Back Propagation 2:

$$\frac{\partial E}{\partial w_{ji}} = \frac{\partial E}{\partial e_k}\frac{\partial e_k}{\partial y_k}\frac{\partial y_k}{\partial u_k}\frac{\partial u_k}{\partial y_i}\frac{\partial y_i}{\partial u_i}\frac{\partial u_i}{\partial w_{ji}} = e_k(-1)f'(u_k)w_{ik}f'(u_i)y_i \tag{A2.29}$$

$$\frac{\partial E}{\partial w_{ji}} = -\left[f'(u_i)\sum_k \delta_k w_{ik} \right] y_j \tag{A2.30}$$

$$\delta_i = f'(u_i)\sum_k \delta_k w_{ik} \tag{A2.31}$$

$$\frac{\partial E}{\partial w_{ji}} = -\delta_i y_j \tag{A2.32}$$

$$\Delta w_{ji} = \lambda \delta_i y_j \tag{A2.33}$$

$$\frac{\partial E}{\partial b_i} = \frac{\partial E}{\partial e_k}\frac{\partial e_k}{\partial y_k}\frac{\partial y_k}{\partial u_k}\frac{\partial u_k}{\partial y_i}\frac{\partial y_i}{\partial u_i}\frac{\partial u_i}{\partial b_i} = e_k(-1)f'(u_k)w_{ik}f'(u_i)(+1) \tag{A2.34}$$

$$\Delta b_i = \lambda \frac{\partial E}{\partial b_i} \tag{A2.35}$$

$$w_{ji}(new) = w_{ij}(old) + \Delta w_{ij} \tag{A2.36}$$

$$b_i(new) = b_i(old) + \Delta b_i \tag{A2.37}$$

Back Propagation 3:

$$\frac{\partial E}{\partial w_{tj}} = \frac{\partial E}{\partial e_k}\frac{\partial e_k}{\partial y_k}\frac{\partial y_k}{\partial u_k}\frac{\partial u_k}{\partial y_i}\frac{\partial y_i}{\partial u_i}\frac{\partial u_i}{\partial y_j}\frac{\partial y_j}{\partial u_j}\frac{\partial u_j}{\partial w_{tj}} = e_k(-1)f'(u_k)w_{ik}f'(u_i)w_{ji}f'(u_j)x_t \tag{A2.38}$$

$$\frac{\partial E}{\partial w_{tj}} = -\left[f'(u_j)\sum_i \delta_i w_{ji} \right] x_t \quad \text{and} \quad \delta_j = \left[f'(u_j)\sum_i \delta_i w_{ji} \right] \tag{A2.39}$$

$$\Delta w_{tj} = \lambda \delta_j x_t \tag{A2.40}$$

$$\frac{\partial E}{\partial b_j} = \frac{\partial E}{\partial e_k}\frac{\partial e_k}{\partial y_k}\frac{\partial y_k}{\partial u_k}\frac{\partial u_k}{\partial y_i}\frac{\partial y_i}{\partial u_i}\frac{\partial u_i}{\partial y_j}\frac{\partial y_j}{\partial u_j}\frac{\partial u_j}{\partial b_j} = e_k(-1)f'(u_k)w_{ik}f'(u_i)w_{ji}f'(u_j)(+1) \tag{A2.41}$$

$$\frac{\partial E}{\partial b_j} = -e_k f'(u_k)w_{ik}f'(u_i)w_{ji}f'(u_j) = -\delta_j \tag{A2.42}$$

$$\Delta b_j = \lambda \delta_j \tag{A2.43}$$

$$w_{ti}(new) = w_{tj}(old) + \Delta w_{tj} \tag{A2.44}$$

$$b_j(new) = b_j(old) + \Delta b_j \tag{A2.45}$$

Steps of the Process:

1) Assign random values to $w_{tj}, b_j, w_{ji}, b_i, w_{ik}, b_k$ for λ >0

2) Calculate the values of y_j, y_i, y_k by using Equations (A2.13-A2.15)

3) Calculate the error by using Equations (A2.11-A2.12)

4) Calculate the values of $\delta_k, \delta_i, \delta_j, \Delta w_{ik}, \Delta w_{ji}, \Delta w_{tj}, \Delta b_k, \Delta b_i, \Delta b_j$

5) Update the weights by using Equations A2.27, A2.28, A2.36, A2.37, A2.44, A2.45

Appendix 3. Learning Rules of the LVQ NN

LVQ learning rule is so called Kohonen learning rule and depends on competition between the process elements in Kohonen layer. Competition depends on calculating the Euclid distance (*d*) between input vector and weight vector (reference vector). The distance for the *i*th process element is calculated by the

$$d_i = \|w_i - x\| = \sqrt{\sum_j (w_{ij} - x_j)^2} \quad \text{(A3.1)}$$

where w_{ij} is the *j*th value of the weight vector and x_j is the *j*th value of the input vector. If the winner process element is the member of the right class, then the new weight vector is recalculated by

$$w(t) = w(t-1) + \lambda(x - w(t-1)) \quad \text{(A3.2)}$$

and otherwise

$$w(t) = w(t-1) - \lambda(x - w(t-1)) \quad \text{(A3.3)}$$

For the y^k is the output of each process element at kohonen layer, then the output for *i*th process element at Kohonen layer y_i^k is equal to one if the process element wins the competition and equal to zero otherwise. The output of the network is calculated by using Equation (A3.4) by multiplying the outputs of process elements at Kohonen layer by the weights that connects these process elements to output layer:

$$y_i = \sum_j y_j^k \alpha_{ki} \quad \text{(A3.4)}$$

where α is the weight of arcs between the output layer and Kohonen layer. The value of α is constant and equals to 1. Equation A3.4 means the output value of the

winner competitive process element of Kohonen layer is equal to one and the output value of other competitive process elements are equal to zero. The process elements in Kohonen layer are connected to only one output element. If the result is true than the reference vector of winner approximated to the input vector as given in Equation (A3.2), and the others are banished as given in Equation (A3.3). These calculations are repeated until all of the samples are correctly (Oztemel, 2003).

Appendix 4. Operation of the CDMM

Before explaining the operation of the CDMM, outputs of the each network are coded as described in Table A4.1. During the operation of CDMM, the outputs that are produced by the members of CNNR are rearranged by 0-1 binary values. For example if the third member of CNNR produces value of two as output, this means that this member's decision is that the pattern shows increasing trend (this numerical code is our assumption). So this result is revaluated as $B_3 = 1$ by CDMM as given at Table A4.1 and the other output values of the third member at CDMM (A_3, B_3, C_3, E_3, and F_3) are revaluated as zero. The detailed information can be refered from (Oztemel, 2003) and (Gauri & Chakraborty, 2008).

Table A4.1 Outputs of the members of CNNR

NN	Output1 NP	Output2 IT	Output3 DT	Output4 DS	Output5 US	Output6 PS
1. Member of CNNR (LVQ)	A_1	B_1	C_1	D_1	E_1	F_1
2. Member of CNNR (LVQ)	A_2	B_2	C_2	D_2	E_2	F_2
3. Member of CNNR (MLP)	A_3	B_3	C_3	D_3	E_3	F_3
Bias1 (For step 1)	$T_1 = 2$					
Bias2 (For step 2)	$T_2 = 2$					

NP: naturel pattern; US: upward shift; DS: downward shift; IT: increasing trend; DT: decreasing trend; PS: periodic shift

The bias values that are given in Table A4.1 represent the minimum number of the members that must produce the same result for collective decision. For example two of three members ($T_1 = 2$) must agree on the same result to accept the result as correct for Step 1. Operation of a CDMM is described below:

Step 1: The outputs that are produced by each NN are summed by matching the same type of outputs together.

$$A = A_1 + A_2 + A_3;\ B = B_1 + B_2 + B_3;\ C = C_1 + C_2 + C_3;\ D = D_1 + D_2 + D_3;$$
$$E = E_1 + E_2 + E_3;\ F = F_1 + F_2 + F_3 \qquad \text{(A4.1)}$$

$$O_x = \max(A, B, C, D, E, F) \quad \text{(A4.2)}$$

If $O_x > T_1$ then set $O_x = 1$ and the others take zero value. For example if $O_x = B$ than this means that a collective decision is performed and a unique solution that takes value of 1 is obtained. The collective decision is that the pattern shows increasing trend (represented by B at Table A4.1) so A, C, D, E, and F takes zero value. The class which has taken value of 1 ($B = 1$) is the collectively decided result. If there are more than one output that are greater than T_1 value or any of the output values does not exceeds T_1 value, then the *Step 2* is performed.

Step 2: The outputs of the NNs are summed by pairs:
For output1:

$$O_{12} = A_1 + A_2;\ O_{13} = A_1 + A_3;\ O_{23} = A_2 + A_3;\ O_{1x} = \max(O_{12}, O_{13}, O_{23}) \quad \text{(A4.3)}$$

$$O_{xx} = \max(O_{1x}, O_{2x}, O_{3x}, O_{4x}, O_{5x}, O_{6x}) \quad \text{(A4.4)}$$

If $O_{xx} > T_2$ then set $O_{xx} = 1$ and the others take zero value. This means a collective decision is performed and a unique solution that takes value of 1 is obtained which means that the presented inputs are belong to the class that the output element's class, which produced value of 1 value (Oztemel, 2003; Gauri & Chakraborty, 2008).

Appendix 5. Learning Rules of the ENN

Topology of ENN is given in Figure A5.1 and Figure A5.2 in detail. It is a recurrent supervised neural network like MLP. But, unlike MLP, it has the dynamic memory property and its input layer does not include transfer function. The ENN employs feedback connections and addresses the temporal relationship of its inputs by maintaining an internal state.

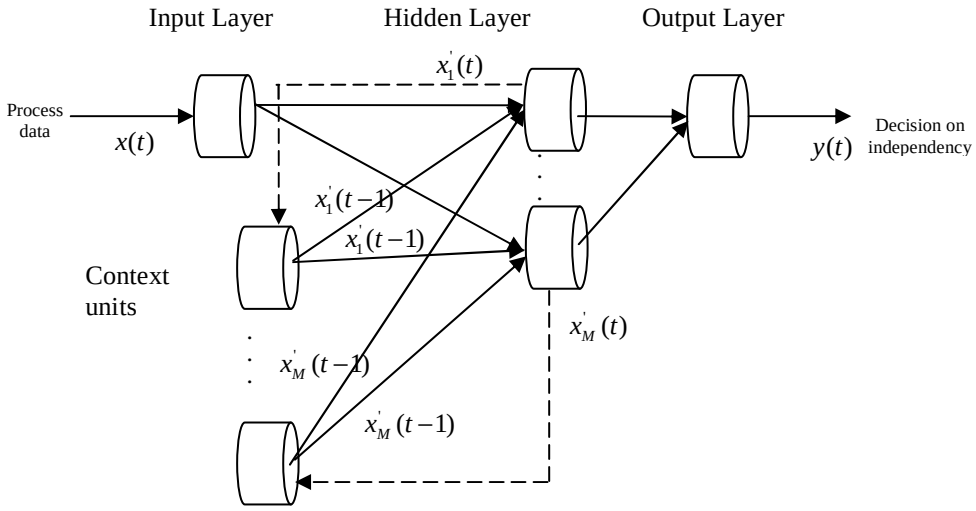

Figure A5.1 An example of a ENN architecture (Ham & Kostanic, 2001; Oztemel, 2003).

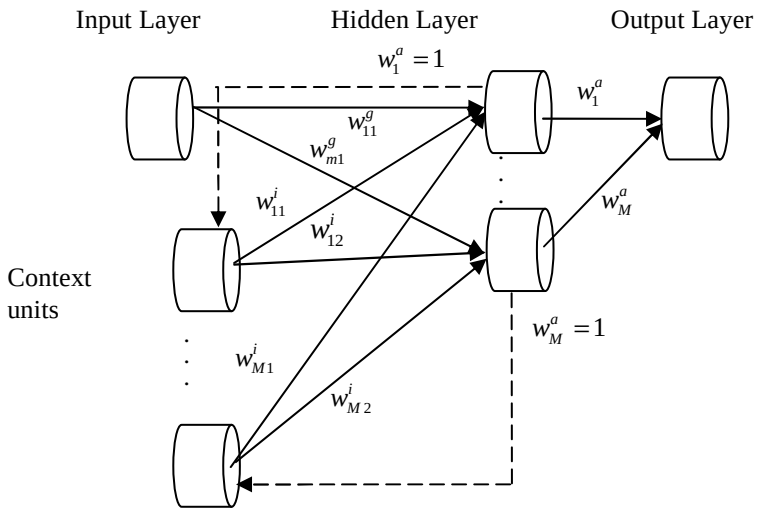

Figure A5.2 Connection weights of Elman NN (Oztemel, 2003).

If the activation function that is used in each time step is sigmoid than the outputs of hidden layer members are calculated by the formula given in Equation (A5.1) (Oztemel, 2003):

$$x_i^{'}(t) = \frac{1}{1+e^{-u_i(t)}} \tag{A5.1}$$

where $u_i(t)$ is the net input for *i*th process element at time step *t*. The net input (u) that is used in Equation (A5.1) is calculated by considering the feedbacks that comes from hidden layer and differs from conventional calculations by MLP learning rules for net input (u) in this aspect. The net input (u) is calculated by the formula given in Equation (A5.2) (Oztemel, 2003).

$$u(t) = w^g x(t) + w^i x^{'}(t-1) \tag{A5.2}$$

If the open form of the formula given in Equation (A5.2) is written, then the Equation (A5.3) is obtained.

$$u_i(t) = \sum_{j=1}^{N} w_{ji}^g x(t) + \sum_{i=1}^{M} w_{ij}^i x^{'}(t-1) \tag{A5.3}$$

where N represents the number of input neurons and M is the number of hidden layer neurons.

The output of the NN is calculated by running the net input (u) value that comes to output element through the linear function. In another words, the activation functions of output elements are linear, so the value of output element that is in output layer at time step t, is calculated by using the weights and the outputs of hidden layer elements as given in Equation (A5.4)

$$y(t) = w^a(t)x^{'}(t) \tag{A5.4}$$

where $w^a(t)$ is the weight and $x^{'}(t)$ is the output of hidden layer elements at time step *t*. The output of *j*th element at time step t is calculated by the Formula given in Equation (A5.5)

$$y_j(t) = \sum_{i=1}^{M} w_i^a(t) x_i^{'}(t) \tag{A5.5}$$

Because of the expected value of the output for each input that is represented to the NN is known, the error occurs at time step t is calculated by

$$e_j = E\left[y_j(t) \right] - y_j(t) \tag{A5.6}$$

where $E\left[y_j(t) \right]$ is the expected output for each input at time step t and e_j is the error occured at time step t. This error term is multiplied by the differention of output value and by this way the error ratios (δ) that will be distributed to weights are determined. The δ that will be distributed to weights at time step t, where the output function is sigmoid, is calculated by the formula given in Equation (A5.7)

$$\delta(t) = y(t) - \left[1 - y(t)\right] E(t) \tag{A5.7}$$

The weight alternation is performed as mentioned at Appendix 2 by the Equation (A2.7) and Equation (A2.8). These alternation values are added to the weights. There is no difference at weight alternation in Elman NN when compared with MLP NN. The weight values of recurrent elements (Context units) are fixed and do not alternates. In other words, while alternating the weight values the weights of context units are not considered. These weights are used to compose the inputs of context units while processing the data forwardly. If the weights of recurrent elements are not considered and the context units are accepted as input elements that Elman network is same as MLP (Oztemel, 2003).

Appendix 6. Abbreviations and Notation

The abbreviations and notations used in this dissertation are as follows:

ξ	Constant of AR(1) process
ϕ	Autoregressive coefficient
ε	Random error term
σ_e	Standard deviation of residuals
d	Trend slope of trend AR(1) process
Z_t	Shifted trend AR(1) process variable
δ_μ	Magnitude of upward mean shift
e_t	Residual (difference between expected and observed values of Z_t)
N	Sample size
β_0	Intercept in a simple linear regression model
β_1	Slope in a simple linear regression model
α	Smoothing constant
σ	Standard deviation of a sample from trend AR(1) process
$\hat{M}_o^t$	Estimated target value for process mean at time t
k	Reference value (allowance, or the slack value)
$\bar{C}^+$	Mean of deviation above $\hat{M}_o^t$
$\bar{C}^-$	Mean of deviations below $\hat{M}_o^t$
UCL_t	Upper control limit for proposed chart at time t
LCL_t	Lower control limit for proposed chart at time t